United States Department of the Interior

BUREAU OF RECLAMATION
P.O. Box 25007
Denver, CO 80225-0007

IN REPLY REFER TO:

86-68110
PRJ-13.00

JUL 1 1 2018

MEMORANDUM

To: Technology Development Program Manager, Dam Safety Office
Attn: 84-44000 (LKrosley)

From: Jerzy Salamon, Civil (Structural) Engineer Stephen J. Dominic for
Waterways & Concrete Dams Group 1

Subject: Transmittal of Dam Safety Technology Development Report DSO-18-10 – Seismically Induced Hydrodynamic Loads on Concrete Dams and Spillway Gates

Attached for your use is the DSO-18-10 Seismically Induced Hydrodynamic Loads on Concrete Dams and Spillway Gates report that has been prepared by the Technical Service Center at the request of the Dam Safety Office. The report will be available in Adobe Acrobat Format on the Dam Safety website and will be loaded into DSDAMS.

If you have any questions, please contact me at 303-445-3219 or via email at JSalamon@usbr.gov.

Hard copy CC recipients:
84-44000 (Dam Safety File Station) (w/att)

Electronic copy CC recipients (w/att):
DSDaMS@usbr.gov
OfficialRecordsArchive@usbr.gov
KBartojay@usbr.gov
LKrosley@usbr.gov
SDominic@usbr.gov
JSalamon@usbr.gov
JEast@usbr.gov

RECLAMATION
Managing Water in the West

Report DSO-18-10

Seismically Induced Hydrodynamic Loads on Concrete Dams and Spillway Gates

Dam Safety Technology Development Program

Technical Service Center
Denver, Colorado

U.S. Department of the Interior
Bureau of Reclamation
Technical Service Center
Denver, Colorado

June 2018

Mission Statements

The U.S. Department of the Interior protects America's natural resources and heritage, honors our cultures and tribal communities, and supplies the energy to power our future.

The mission of the Bureau of Reclamation is to manage, develop, and protect water and related resources in an environmentally and economically sound manner in the interest of the American public.

REPORT DOCUMENTATION PAGE		*Form Approved* *OMB No. 0704-0188*
T1. REPORT DATE: JUNE 2018	**T2. REPORT TYPE:** TECHNICAL	**T3. DATES COVERED** June 2018
T4. TITLE AND SUBTITLE Seismically Induced Hydrodynamic Loads on Concrete Dams and Spillway Gates		**5a. CONTRACT NUMBER** **5b. GRANT NUMBER** **5c. PROGRAM ELEMENT NUMBER**
6. AUTHOR(S) Jerzy W. Salamon, Ph.D., P.E, Denver, CO (BOR, 303 445 3219)		**5d. PROJECT NUMBER** DSO-2018-10 **5e. TASK NUMBER** **5f. WORK UNIT NUMBER** HYLS8
7. PERFORMING ORGANIZATION NAME(S) AND ADDRESS(ES) Department of the Interior, Bureau of Reclamation Technical Service Center, Denver Federal Center PO Box 25007 (86-68110) Denver, CO 80225-0007		**8. PERFORMING ORGANIZATION REPORT NUMBER**
9. SPONSORING / MONITORING AGENCY NAME(S) AND ADDRESS(ES) Department of the Interior, Bureau of Reclamation Dam Safety Office, Denver Federal Center PO Box 25007 (84-44000) Denver, CO 80225-0007		**10. SPONSOR/MONITOR'S ACRONYM(S)** **BOR/USBR:** Bureau of Reclamation **DOI:** Department of the Interior **DSO:** Dam Safety Office **11. SPONSOR/MONITOR'S REPORT NUMBER(S)** **DSO-2018-10**
12. DISTRIBUTION / AVAILABILITY STATEMENT		
13. SUPPLEMENTARY NOTES		

14. ABSTRACT In the report, three methods that are commonly used in the time analysis of the dam-reservoir-foundation system during an earthquake are evaluated. These include: the "added mass", the "acoustic fluid", and the "fluid-like material model" methods. The theory for each of the methods is briefly presented and it is illustrated by the results for a case of two concrete dams and a large radial gate.

15. SUBJECT TERMS :

16. SECURITY CLASSIFICATION OF: UU			**17. LIMITATION OF ABSTRACT:** SAR	**18. NUMBER OF PAGES** 34 (excluding Appendix)	**19a. NAME OF RESPONSIBLE PERSON:** Jerzy Salamon
a. REPORT UU	**b. ABSTRACT** UU	**c. THIS PAGE** UU			**19b. TELEPHONE NUMBER** 303 445 3219

S Standard Form 298 (Rev. 8/98)
P Prescribed by ANSI Std. 239-18

BUREAU OF RECLAMATION
Technical Service Center, Denver, Colorado

Report No. DSO-18-10

Seismic Induced Hydrodynamic Loads on Concrete Dams and Spillway Gates

JERZY SALAMON Digitally signed by JERZY SALAMON
Date: 2018.06.25 09:01:22 -06'00'

Prepared by: Jerzy Salamon, Ph.D., P.E.
Waterways & Concrete Dams Group 1, 86-68110

HILLERY VENTURINI Digitally signed by HILLERY VENTURINI
Date: 2018.06.26 08:35:27 -06'00'

Checked by: Hillery Venturini, P.E.
Waterways & Concrete Dams Group 1, 86-68110

JERZY SALAMON Digitally signed by JERZY SALAMON
Date: 2018.06.25 09:01:53 -06'00'

Technical Approval: Jerzy Salamon, Ph.D., P.E.
Waterways & Concrete Dams Group 1, 86-68110

LAN NGUYEN Digitally signed by LAN NGUYEN
Date: 2018.06.25 09:09:09 -06'00'

Peer Review by: Lan Nguyen, Ph.D., P.E. Date
Waterways & Concrete Dams Group 1, 86-68110

REVISIONS

Date	Description	Prepared	Checked	Technical approval	Peer review

CONTENTS

I. Introduction 1
- A. Background 1
- B. Purpose and scope of work 1

II. Analysis of Dam-Reservoir-Foundation System 2
- A. General 2
- B. Westergaard's Approach 3
- C. Acoustic Fluid Approach 8
- D. Fluid-Like Behavior Model 10

III. Constitutive Model of Water 11
- A. General 11
- B. Compressibility of Fluid 11
- C. Viscosity of water 12

IV. Case Studies - Gravity Dams 13
- A. General 13
- B. Description of the FE Model 13
- C. Modal Analysis 14
- D. Time Analysis 15

V. Spillway Radial Gate - Case Study 18
- A. General 18
- B. FE Model of Radial Gate 18

VI. Reservoir-Gate-Dam System 20
- A. General 20
- B. Spillway Gate Set-back Effect 21
- C. Comprehensive Analysis of the Gate–Dam-Reservoir System 23

VII. Conclusions 24
- A. Summary 24
- B. Conclusions 24
- C. Future Research 25

IX. References 26

X. Appendix 27

I. Introduction

A. Background

Hydrodynamic loads induced during earthquakes are of importance in the design of new dams and structural assessment of existing concrete dams and the dam appurtenant structures. In-depth understandings of the computation methods, their limitations, and proper interpretation of the analysis results are the key factors that determine confidence in the solution and the accuracy of the analysis results.

During the 2016 Monticello Blind Prediction Analysis Workshop hosted by the United States Society on Dams (USSD) Committee on Concrete Dams and the Earthquake Committee, a case study for Monticello Dam was investigated. At the workshop, participants attempted to replicate the response of the arch dam for the provided field measured seismic loads using various finite element (FE) software. Significant differences were observed among the presented results. One of the primary reasons for the differences observed in the results provided by the participants appears to be the various computation approaches used to determine the hydrodynamic loads induced during earthquakes, namely: the “added mass” approach, the “acoustic fluid” formulation, and the “fluid-like material model” technique.

Upon observation of the workshop, there is a need to review the concept of each approach, perform case studies, and summarize the results as well as draw out the conclusions from the study. This report therefore, documents the literatures based upon the reviewing process, describes the case studies performed for the approaches mentioned above, and finally provides the conclusions drawn from the results.

B. Purpose and scope of work

The purpose of this Technical Memorandum (TM) is to:

1) present a concept of the analysis methods that are commonly used in the computation practice to determine seismically induced hydrodynamic loads on concrete dams.

2) document case studies for concrete gravity dams and spillway radial gates to illustrate application of the discussed analysis methods.

II. Analysis of Dam-Reservoir-Foundation System

A. General

Analysis Flowchart

One of the primary goals of a seismic analysis for concrete dams or spillway gates is to determine the response of the structure to the applied loads. Analysis results in the form of displacements, strains, and stresses are used to assess the structural conditions and to evaluate the structural stability and safety of the structure.

In general, the process for the dam-reservoir-foundation model analysis for seismic loads could be presented in following stages (a flow chart is presented in Figure 1):

- Identifying a **real object** of interest.
- Developing a **physical model**: at this stage, nominal dimensions, characteristic material properties, and load models are determined.
- Formulating a **mathematical model**: for the given physical model, a system of mathematical equations is defined that describes a response of the structure to the applied loads. In the structural analysis of concrete dams, the mathematical model could be as simple as a formula describing behavior of a "rigid block" or as advanced as a system of partial differential equations describing a nonlinear behavior of the physical model for seismic loads.
- Analytical calculations of numerical **solution** of the mathematical problem: for solving the complex mathematical model, the use of a specialized software is required.
- **Interpretation** of the analysis results: a non-linear problem formulation introduces stress and strain measures that are not common in engineering practice. Proper interpretation of such measures and developing engineering understandings of them is of high importance.
- **Verification** of the results: it is important to note that the numerical solutions are only <u>approximations</u> of the exact solutions. An estimate of the <u>solution error</u> whenever a numerical analysis is conducted is required.
- **Model refinement**: based on the accuracy verification of the solution, the mathematical model or the solution model, may need to be refined to obtain a more accurate solution.
- **Presentation** of the analysis results: after a confidence level in the solution is achieved, the analysis could be considered complete and the results can be presented with confidence.

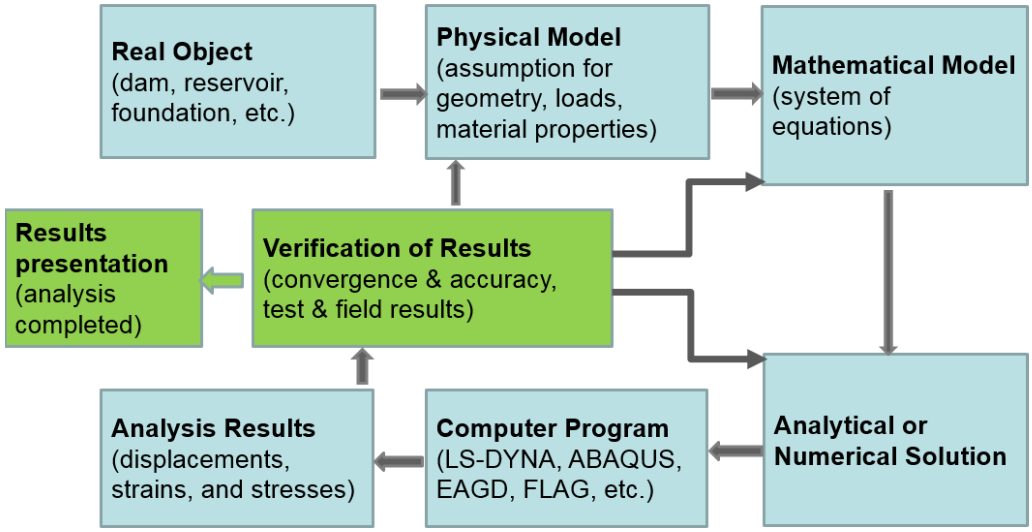

Figure 1. Flowchart – analysis procedure [1].

Complexity of the Analysis

Complexity of the mathematical models for the dam-reservoir-foundation system in seismic analysis is associated with the following aspects:

- Loads: static, pseudo-static, or time-dependent loads.
- Contact with friction introduces a non-linearity to the model: opening of contraction joints or sliding of the dam at foundation interface.
- Material behavior: linear, non-linear, failure, age and temperature dependent materials associated with a relation between strains and stresses.
- Large deformation associated with non-linear relations between displacements and strains.
- Non-reflecting boundary conditions, which numerically prevent the artificial stress wave reflection generated at the model boundaries from “reentering” the model and contaminating the results.
- Interaction between a dam and a reservoir. The mathematical model of the seismically induced hydrodynamic interaction in the dam – reservoir system could be as simple as described by the Westergaard’s “added mass” formulation, or as complex as the time dependent coupled system of partial differential equations formulated for the dam, the foundation, and the reservoir.

B. Westergaard’s Approach

1. General

The first systematic approach for a dam-reservoir interaction analysis was developed by Westergaard [2] in 1932 in connection with the design of Hoover Dam by the Bureau of Reclamation (Reclamation) and was followed by Zanger in

Reclamation's laboratory [3]. In a study of the earthquake response of a rigid dam with a vertical upstream face (Figure 2), Westergaard developed an analytical solution of the hydrodynamic pressure distribution in the reservoir and along the upstream face of the dam for a harmonic horizontal motion of the dam. Based on this exact solution, an approximate formula, in a form of a parabolic hydrodynamic pressure distribution at the dam face was developed. It was formulated in such fundamental and simplistic form, that it has been consistently used in the engineering practice in a preliminary analysis and design of concrete dams to date.

2. Problem Formulation

Seismic motions of a straight rigid concrete gravity dam interacting with an infinite length reservoir of depth, *h*, shown in Figure 2, were mathematically described by Westergaard [2] in terms of the theory of elasticity of solids based on the formulation provided by H. Lamb in *Hydrodynamics* in 1924. Equations of motions, a linear kinematic relation for small deformations, and an elastic constitutive equation, coupled with the boundary conditions (dynamic pressure equal zero at the reservoir surface, vertical displacement equal zero at the bottom of the reservoir) described the two-dimensional physical model of the dam-reservoir system.

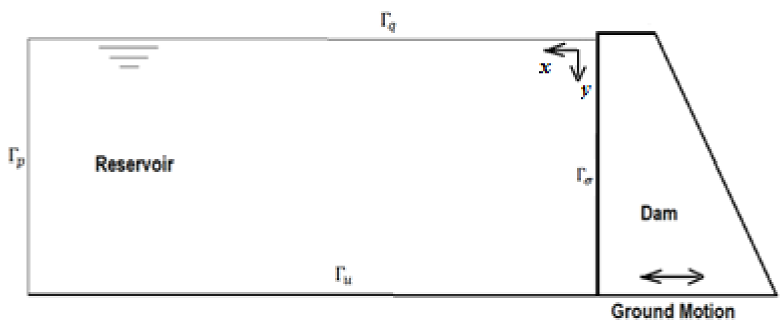

Figure 2. Westergaard's physical model.

The mathematical model was formulated by Westergaard by:

Equations of Motion:

$$\frac{\partial \sigma}{\partial x} = \frac{w}{g}\frac{\partial^2 u}{\partial t^2} \qquad \frac{\partial \sigma}{\partial y} = \frac{w}{g}\frac{\partial^2 v}{\partial t^2} \qquad \text{(Eq.1)}$$

Geometric Equations:

$$\varepsilon_{xy} = \frac{1}{2}\left(\frac{\partial u}{\partial y} + \frac{\partial v}{\partial x}\right) \qquad \text{(Eq.2)}$$

Constitutive Law for Reservoir:

$$p = \tfrac{1}{3}\sigma_{kk} = K\,\varepsilon_{kk} \qquad \text{(Eq.3)}$$

where: *u*, *v* are horizontal and vertical displacements, respectively

x is the axis at the surface of the water directed upstream (Figure 2)
y is the vertical downward axis (Figure 2)
p is the pressure in the reservoir
σ_{kk} *and* ε_{kk} are volumetric stress and volumetric strains
w is the weight of water per unit of volume
g is the acceleration due to gravity
K is the bulk modulus of water

In Westergaard's original form, the following assumptions were made:

- The problem is defined in two-dimensional (2D) space
- The dam upstream face is straight and vertical at Γ_σ
- The dam does not deform, is considered to be a rigid block. Westergaard assumed that the period of free vibration of the dam, T_0, is significantly smaller than the period of the earthquake (no resonance).
- The reservoir is infinite in length at Γ_p
- Small motions are assumed during earthquake
- Non-dimensional horizontal acceleration of $\alpha = 0.1$ was assumed
- Sinusoidal oscillations of the dam are horizontal

3. *Exact Solution*

The solution of the boundary value problem (plane strain) was given by Westergaard in the form of a stress (pressure) distribution in the reservoir by Eq.4.

$$\sigma = -\frac{8\alpha wh}{\pi^2}\cos\frac{2\pi t}{T}\sum_{1,3,5\ldots}^{n}\frac{1}{n^2 c_n}e^{-q_n}\sin\frac{n\pi y}{2h}$$

(Eq.4)

$$q_n = \frac{n\pi c_n x}{2h} \qquad c_n = \sqrt{1 - \frac{16wh^2}{n^2 gkT^2}}$$

According to Eq. 4, the maximum pressure p occurs when the dam is in the extreme positions (at time of t = 0, T, 2T, etc.) during motion, so the maximum water pressure distribution at the upstream face of dam (for x =0, q_n = 0) could be expressed by Eq.5:

$$p = \frac{8\alpha wh}{\pi^2}\sum_{1,3,5\ldots}^{n}\frac{1}{n^2 c_n}\sin\frac{n\pi y}{2h}$$ (Eq.5)

$$c_n = \sqrt{1 - \frac{16wh^2}{n^2 gkT^2}}$$

where: w = weight of water per unit volume (w = 62.4 lb/ft^3)
g = acceleration due to gravity (g = 32.2 ft/sec^2)
α = maximum horizontal acceleration of foundation divided by g
T = period of horizontal vibration of the dam,
t = time (seconds)

k = bulk modulus of water (k = 300,000 lb/ft^2)

4. Approximate Solution

An approximate formula in a form of a parabolic function, developed using the exact solution (Eq.5), describes the pressure at the face of the dam by (Eq.6):

$$p = \frac{7}{8} w\alpha \sqrt{h(h-y)} \qquad \text{(Eq.6)}$$

5. Concept of Added Mass

Westergaard also introduced in his 1932 publication a concept of *"added mass"*. He defined this concept as "a mass of a certain body of water which was forced to move with the dam during the ground motion". The volume of water of "*added mass*" per unit width was described by a parabola with the width "*b*" expressed by Eq.7. The graphical representation of Eq.7 is presented in Figure 3:

$$b = \frac{7}{8} w \sqrt{h(h-y)} \qquad \text{(Eq.7)}$$

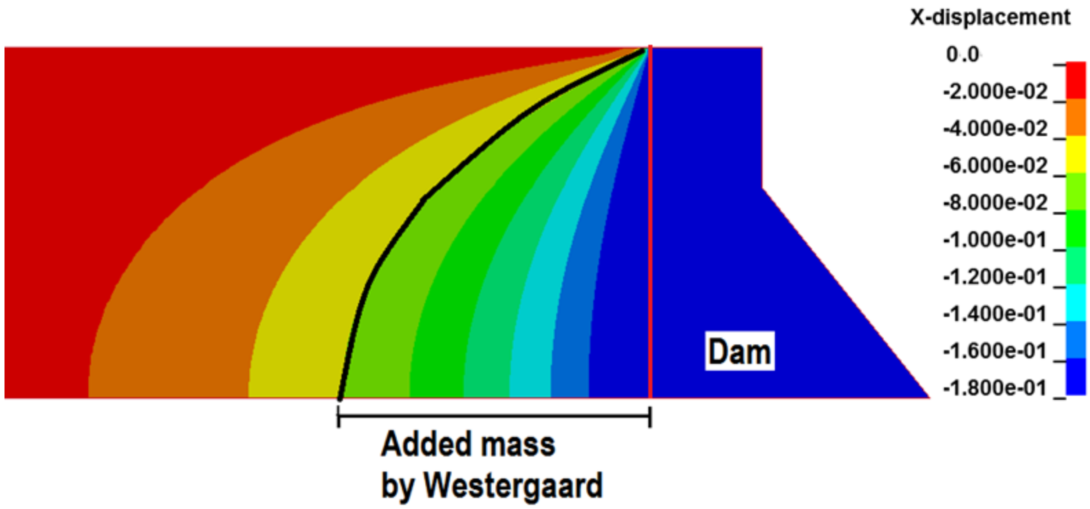

Figure 3. Horizontal displacements of a rigid dam obtained in FE analysis for a 100-foot-deep reservoir. Black line denotes the width "*b*" of *added mass* volume determined by Westergaard, per Eq.7.

6. Comparison of Westergaard's Results

General

In this section, Westergaard's exact and approximate solutions are compared with FE analysis results. For the purpose of the study, a spreadsheet was developed to calculate the pressure distribution at the face of the dam for both of Westergaard's formulas. The spreadsheet was calibrated with the results provided in the original Westergaard's paper [2] for reservoir depths of 200, 400, and 600 feet, with the period of horizontal dam vibrations, *T*, between 0.33 and 4 seconds. The results are presented in this section for a case of a 100-foot-deep reservoir.

Reservoir natural frequency

The first natural frequency of the reservoir can be determined by the equation:

$$f_r = \frac{c_w}{4\,h} \qquad \text{(Eq.8)}$$

For the 100-foot-deep reservoir, the natural frequency of the reservoir (Eq. 8) is 12.18 Hz, and the corresponding period of vibration is 0.082 seconds.

Results for Westergaard Solutions

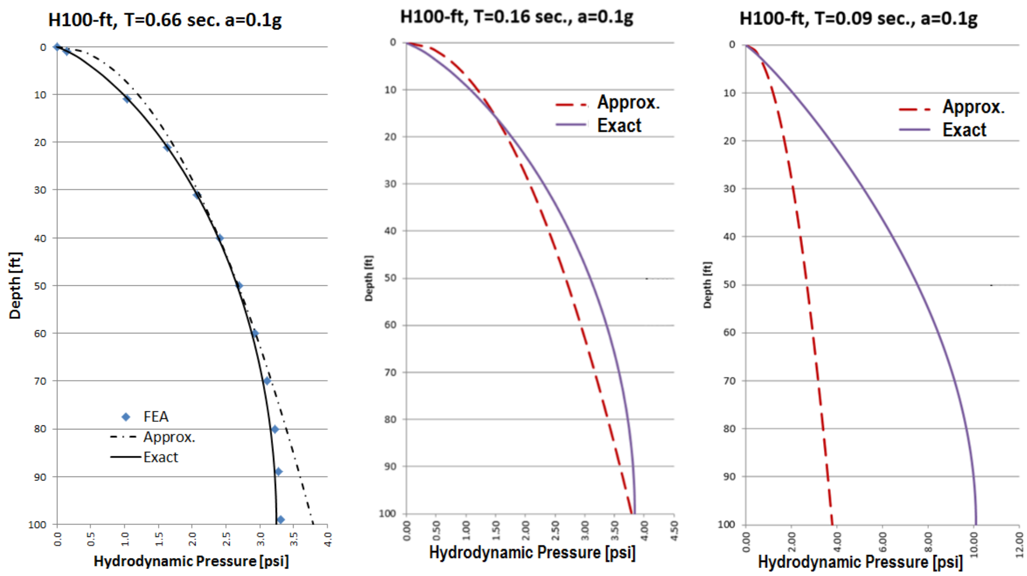

Figure 4. Hydrodynamic pressures at the face of a 100-foot-high rigid dam obtained by exact and approximate Westergaard's solutions for the harmonic dam excitations at periods of 0.66 seconds (1.52 Hz), 0.16 seconds (6.25 Hz), and 0.09 seconds (11.1 Hz) and the acceleration amplitude of 0.1g.

Agreement can be observed between the exact Westergaard's solution and the FE analysis results for the excitation period of 0.66 seconds (Figure 4 – left). As the dam excitation period approaches the first natural frequency of the reservoir of 0.082 seconds (Eq. 8), the exact Westergaard's solution deviates from the approximate solution which remains constant (i.e. excitation frequency independent). The increase in hydrodynamic pressure determined by the exact Westergaard's solution (Figure 4, right) could be explained by the resonance interaction between the reservoir (i.e. first natural frequency of 12.18 Hz) and the dam excitation frequency of 11.1 Hz. This confirms that the Westergaard's solution is valid when the frequency of excitations differs from the first natural frequency of the reservoir.

It was also observed that the approximate Westergaard's formula (Figure 4 – left) overestimates the hydrodynamic pressure at the upper part of a rigid dam, where the spillway is located, when compared with the exact Westergaard's solution and the FE analysis results.

C. Acoustic Fluid Approach

1. General

This section presents a brief overview of the "acoustic fluid" formulation used in the seismic simulation of the dam-reservoir systems.

2. Coupling of Acoustic Fluid and Structural Elements

In this approach, the displacement field of the dam (structural domain, or "Solid" in Figure 5) is coupled with the pressure field of the reservoir (fluid domain, or "Fluid" in Figure 5) via the interaction forces at the interface Γ_I between the dam and the reservoir (Figure 5).

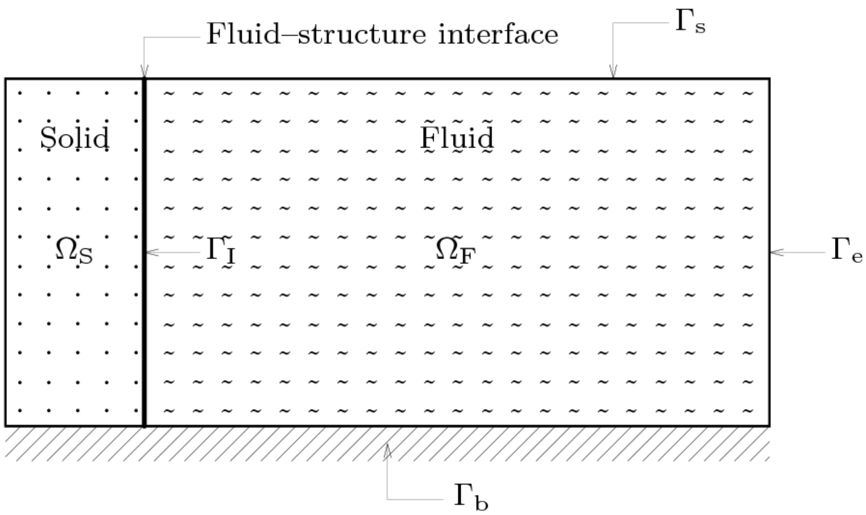

Figure 5. Coupled model of an acoustic fluid and a solid.

In the structural domain Ω_S, the discretization is given by:

$$\mathrm{M_S}\ddot{u} + \mathrm{C_S}\dot{u} + \mathrm{K_S}u + \mathrm{f_I} = \mathrm{f_S^{ext}} \quad \text{(Eq.9)}$$

where: $\mathrm{M_S}$, $\mathrm{C_S}$, and $\mathrm{K_S}$ = mass, damping, and stiffness matrices, respectively
u = displacements in the structural domain
$\mathrm{f_I}$ = forces due to the interface interaction with the fluid
$\mathrm{f_S^{ext}}$ = external forces

The dynamic pressure distribution in the fluid is described by a single variable p. Assuming the state of the fluid is linear (compressibility of the fluid is considered), the governing equation is the wave (acoustic) equation:

$$\nabla^2 p = \frac{1}{c^2}\ddot{p} \quad \text{(Eq.10)}$$

where: p = dynamic pressure (compression positive)
c = wave velocity given by Eq.11:

$$c^2 = \frac{K}{\rho_F} \tag{Eq.11}$$

where: K = bulk modulus of fluid
ρ_F = fluid density

Coupling of the dam and the reservoir is achieved by considering the interface forces at the dam face. The conditions applied to the fluid-structure interface Γ_I can be written as:

$$\sigma\, n_S = p\, n_F \tag{Eq.12}$$

where: n_F and n_s = outward normal to the fluid domain and the outward normal to the structural domain, respectively.

Coupling between the structural domain and the fluid domain can be achieved by continuity between the normal displacements with the condition $u_F = u_S$ and is obtained by combining this condition with Eq.12 as:

$$\frac{\partial p}{\partial n} = -\rho_F \mathrm{n_F}^{\mathrm{T}} \ddot{\mathrm{u}}_{\mathrm{S}} \tag{Eq.13}$$

At the free surface, Γ_s, and the fluid far field boundary (infinite extent), Γ_e, the prescribed dynamic pressures are assumed zero. For the bottom boundary, Γ_b, a full reflective or partial wave reflection could be assumed.

Implementing a standard FE discretization for approximating pressure, p, a system of algebraic equations for the fluid domain can be expressed by:

$$\mathrm{M_F}\ddot{\mathrm{p}} + \mathrm{K_F}\mathrm{p} + \mathrm{r_I} = 0 \tag{Eq.14}$$

where: $\mathrm{M_F}$ and $\mathrm{K_F}$ = fluid mass and stiffness matrixes, respectively
$\mathrm{r_I}$ = interface reaction force.

The interface interaction forces within the fluid element can be written as:

$$f_I^e = -R^{eT} p^e \tag{Eq.15}$$

where: R^e = interaction matrix for the dynamic pressures on the element level.

Likewise, the contribution r_I on the element level is:

$$r_I^e = \rho_F R^e \ddot{u}^e \qquad \text{(Eq.16)}$$

After assembling contributions from each type of element, the following coupled system of equations for the fluid structure interaction problem is obtained:

$$\begin{bmatrix} M_S & 0 \\ \rho_F R & M_F \end{bmatrix} \begin{Bmatrix} \ddot{u} \\ \ddot{p} \end{Bmatrix} + \begin{bmatrix} C_S & 0 \\ 0 & 0 \end{bmatrix} \begin{Bmatrix} \dot{u} \\ \dot{p} \end{Bmatrix} + \begin{bmatrix} K_S & -R^T \\ 0 & K_F \end{bmatrix} \begin{Bmatrix} u \\ p \end{Bmatrix} = \begin{Bmatrix} f_S^{ext} \\ 0 \end{Bmatrix} \qquad \text{(Eq.17)}$$

If the compression effects are neglected (i.e., an incompressible fluid is assumed, the fluid matrix M_F becomes zero. The dynamic pressure vector **p** can now be obtained directly in terms of $\ddot{u}$ as:

$$\mathbf{p} = -K_F^{-1} \rho_F R \ddot{u} \qquad \text{(Eq.18)}$$

Combining Eq. 17 in Eq. 16, the structural matrix results in the following general equation:

$$\left(M_S + \widetilde{M}_F\right)\ddot{u} + C_S \dot{u} + K_S u = f_S^{ext} \qquad \text{(Eq.19)}$$

where the added mass is simply given by:

$$\widetilde{M}_F = \rho_F R^T K_F^{-1} R \qquad \text{(Eq.20)}$$

If an arbitrary transient loading is considered, the response of the model with incompressible fluid is obtained by a direct time integration method.

The "acoustic fluid" structural element approach is implemented in the DIANAFEA software developed by DIANA FEA [4].

D. Fluid-Like Behavior Model

1. Problem Formulation

In the continuum theory of mechanics, the set of basic equations that includes equations of motions (Eq.21), geometric equations (Eq.22), and material constitutive law (Eq.23 and Eq.24), together with boundary and initial conditions (Eq.25 and Eq.26), defines a mathematical formulation of the dynamic problem for linear elastic materials of fluid and concrete.

Modeling fluid behavior with a "fluid-like" material model is an alternative approach for analyzing the fluid-structure interaction behavior. The fluid is defined as a structural elastic material (Eq.24) with the shear modulus for water equal to zero.

Equations of motion: $\sigma_{ij,j} + \rho b_i = \rho \ddot{u}_i \qquad i,j,k = 1,2,3 \qquad$ (Eq.21)

Geometric equation: $\varepsilon_{ij} = \frac{1}{2}\left(u_{i,j} + u_{j,i} + u_{k,i}u_{k,j}\right) \qquad$ (Eq.22)

Constitutive law for solid: $\sigma_{ij} = \frac{E}{1+\nu}\left(\varepsilon_{ij} + \frac{\nu}{1-2\nu}\varepsilon_{kk}\delta_{ij}\right)$ (Eq.23)

Constitutive law for fluid $\dot{p} = \frac{1}{3}\dot{\sigma}_{kk} = K\,\dot{\varepsilon}_{kk}$ (Eq.24)

where: $\underline{u}$, $\underline{\varepsilon}$, $\underline{\sigma}$, p = displacement, strain, stress tensors, and pressure, respectively
ρ, b =mass density and body force, respectively
E, ν, K = elastic modulus and Poisson ratio of concrete, and bulk modulus of fluid, respectively.
$\dot{\varepsilon}, \dot{\sigma}, and\ \dot{p}$ = strain, stress, and pressure rates, respectively

Boundary Conditions:

$$\begin{aligned} &\sigma_{ij}n_j = T_i && on\ \Gamma_\sigma \\ &\bar{q} = 0 && on\ \Gamma_q \\ &u_i = 0 && on\ \Gamma_u \\ &p = \bar{p} && on\ \Gamma_p \end{aligned} \quad \text{(Eq.25)}$$

where Γ_σ, Γ_q, Γ_u, Γ_p are parts of the boundary shown in Figure 2.

Initial Conditions:

$$u_i(x,t_0) = u_i^0(x) \qquad \dot{u}_i(x,t_0) = v_i^0(x) \qquad \ddot{u}_i(x,t_0) = a_i^0(x) \quad \text{(Eq.26)}$$

The fluid-like material model is implemented in LS-DYNA software developed by LSTC [5].

III. Constitutive Model of Water

A. General

In general, total deformations could be expressed by two components: deviatoric (relative shape change) and axiatoric (relative volume change as a response to pressure changes):

$$\Delta\varepsilon_{ij} = \Delta\varepsilon'_{ij} + {}^{1}\!/_{3}\,\Delta\varepsilon_{kk}\delta_{ij} \quad \text{(Eq.27)}$$

where:

$\Delta\varepsilon_{ij}'$ = deviatoric strain increment
$\Delta\varepsilon_{kk}$ = axiatoric strain increment

The axiatoric component describes compressibility and the deviatoric component describes viscosity of the fluid properties.

B. Compressibility of Fluid

The volumetric compression in fluid is within elastic linear deformation range and could be expressed for water in form of the Polynomial Equation-of-State (EOS) by:

$$p = C_0 + C_1\mu = C_0 + K\mu = C_0 + K\,\frac{v_0 - v}{v} \qquad \text{(Eq.28)}$$

where:

C_0 = initial pressure (atmospheric pressure),
C_1 = bulk modulus, K_{water}

Table 1 lists selected, typical values of water density and compressibility. Both properties vary with the pressure and temperature.

Table 1 – Selected values of water properties

Typical Constant Values	**Symbol**	**Units**	
		[Kg-m-s-K]	[lbf/(in/s^2)-in-s-R]
Water density at 70°F	ρ_{water}	998.0 Kg/m^3	9.34E-5 lbf/(in/s^2)in^3
Water bulk modulus at pressure 15 psi & 58°F	K_{water}	2.15E9 Pa	312,0000 lbf/in^2

C. Viscosity of water

Viscosity is the fundamental characteristic property of all fluids. It is usually defined as the measure of internal friction or resistance of the fluid. Viscosity can be expressed by dynamic viscosity named as *absolute viscosity*. In general, it is a tangential force per unit area, which is required to drag one layer of fluid to another. Mathematically, the above described phenomena can be written in the differential form as:

$$\Delta\sigma' = \mu' \frac{\partial u}{\partial x} = \mu' \Delta\dot{\varepsilon}' \qquad \text{(Eq.29)}$$

where:

$\Delta\sigma'$ = deviatoric (viscous) stress
μ’ = dynamic viscosity
∂u/∂y = velocity gradient
$\Delta\dot{\varepsilon}'$ = deviatoric strain rate.

Table 2 – Typical values of dynamic viscosity of water [Lide D.R., *CRC Handbook of Chemistry and Physics*, CRC Press, 2004]

Temperature	**Dynamic Viscosity (Pa s)**	**Dynamic Viscosity (*lb$_f$ s/ft^2*)**
0 ^{o}C (32^{o}F)	0.001787	0.0000373
5^{o}C (41^{o}F)	0.001519	0.0000319
10^{o}C (50^{o}F)	0.001307	0.0000273
20^{o}C (68^{o}F)	0.001002	0.0000210

Although the viscous property of water is generally neglected in the analysis of reservoir dam interaction problems, its consideration could help in convergence of the numerical solutions.

IV. Case Studies - Gravity Dams

A. General

To illustrate the differences from the analysis techniques discussed above, two concrete dam models were investigated [6]: (1) a small 100-foot-high dam (Figure 6 – left), and (2) a medium size 287-foot-high dam (Figure 6-right). The foundation in both models has a length of 1,200 feet and a depth of 300 feet. For this comparison study, the foundation is modeled as a massless rigid or with linear elastic material properties. The water level is 100 feet (to the top of the dam crest) for the small dam, and 282 feet for the medium dam. The reservoir has an upstream length of 600 feet for both dam models.

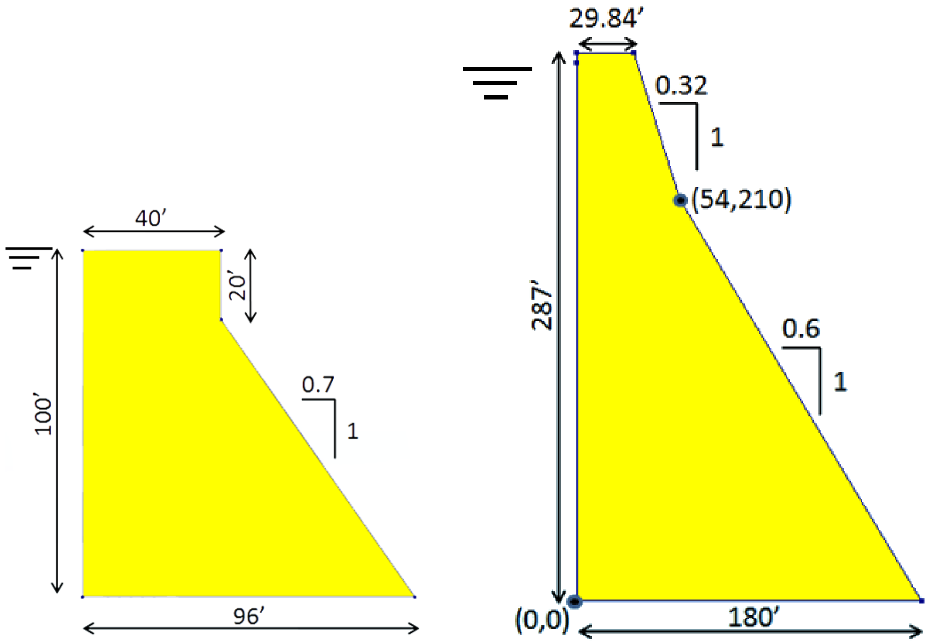

Figure 6. Model geometry of small dam (left) and medium size dam (right).

B. Description of the FE Model

The FE models for both cases are defined in plane strain formulation. At the free surface, and the fluid far field boundary (infinite extent), the prescribed dynamic pressures are defined as zero. For the reservoir bottom, a full reflective boundary is assumed (i.e. no bottom absorption effects or prescribed dynamic pressures). Table 3 lists the material properties used in the analysis for the dam, foundation, and reservoir.

Table 3. Material properties selected for the analysis; (* - Bulk modulus value)

Material property	Dam	Foundation	Reservoir	Unit
Young's modulus E	4.0E6	3.0E6	3.0E5*	lb/in^2
Poisson's ratio ν	0.2	0.2	-	-
Density ρ	155.0	0.0	62.4	lb/ft^3
Sonic speed c_w	-	-	4,869.0	ft/s

The amplitude of the excitation (i.e. prescribed harmonic acceleration in horizontal direction) was 0.1 g and was applied at the base of the dams for the model with a rigid foundation, and at the bottom and sides of the foundation blocks for the model with the elastic properties of the foundation. The harmonic excitations at 0.66 second and 1.33 seconds were considered in the analysis.

C. Modal Analysis

The ratio of the natural frequency of the reservoir to the natural frequency of the dam is a key parameter describing the effect of the reservoir compressibility in the reservoir-dam interaction during an earthquake [6]. The first natural frequency of the reservoir can be determined for reservoir depths of 100 feet and 282 feet from Eq. 8. These natural frequencies for the small and medium dam models (Figure 6) are 12.18 Hz and 4.32 Hz, respectively.

Four eigenfrequencies for the small size dam and medium size dam models are presented in Tables 4 and 5, respectively. The frequencies were determined by free-vibration eigenvalue analyses for the empty reservoir, added mass, and incompressible fluid case, and by a direct frequency response method for the compressible fluid case, considering elastic and rigid foundations.

Table 4. Eigenfrequencies [Hz] for small size dam.

Reservoir	Foundation	1st	2nd	3rd	4th
Empty reservoir	rigid	13.1	32.0	33.9	61.8
Empty reservoir	elastic	8.2	15.2	21.6	43.4
Added mass	rigid	11.5	28.7	32.2	50.9
Added mass	elastic	7.1	15.1	19.1	39.1
Incompressible fluid	rigid	11.9	30.2	32.4	58.9
Incompressible fluid	elastic	7.3	15.1	20.1	42.4
Compressible fluid	rigid	11.0	28.7	31.5	50.1
Compressible fluid	elastic	7.1	15.1	20.7	42.2

Table 5. Eigenfrequencies [Hz] for medium size dam.

Reservoir	Foundation	1st	2nd	3rd	4th
Empty reservoir	rigid	3.9	10.0	12.9	18.6
Empty reservoir	elastic	2.9	7.1	8.1	13.2
Added mass	rigid	3.0	7.8	12.8	14.3
Added mass	elastic	2.3	6.0	7.8	11.2
Incompressible fluid	rigid	3.2	8.6	12.8	17.0
Incompressible fluid	elastic	2.4	6.5	7.8	13.1
Compressible fluid	rigid	3.1	5.0	7.3	9.4
Compressible fluid	elastic	2.4	4.9	6.6	12.3

The results presented in Tables 4 and 5 show that the eigenfrequencies of the dam- reservoir-foundation system vary significantly with the type of the dam-reservoir-foundation model considered in the analysis. The highest natural frequency is obtained for the elastic dam model on rigid foundation without the presence of the reservoir. Note that elasticity of the foundation is a significant factor influencing the natural frequency of the dam-reservoir-foundation system.

Table 6 presents the ratios between natural frequencies of the reservoir and natural frequencies of the dam-reservoir-foundation model.

Table 6. Ratio between the first natural frequencies of the reservoir and the dam-reservoir-foundation model.

Reservoir	Foundation	Small Size Dam	Medium Size Dam
Empty reservoir	rigid	0.93	1.11
Empty reservoir	elastic	1.49	1.49
Added mass	rigid	1.06	1.44
Added mass	elastic	1.72	1.87
Incompressible fluid	rigid	1.02	1.35
Incompressible fluid	elastic	1.67	1.80
Compressible fluid	rigid	1.11	1.39
Compressible fluid	elastic	1.72	1.80

In general, the first natural frequency of the reservoir is higher than that of the dam-reservoir-foundation system for both dam models (ratio larger than 1.0 in Table 6).

D. Time Analysis

The time analyses were also performed using the "fluid-like material model" approach [5], with two scenarios: rigid (i.e. no) foundation and elastic material foundation for the dam-reservoir-foundation system. A rigid foundation was assigned with harmonic excitation of the dam at periods of 0.66 second and 1.33 seconds. Figures 7 and 8 present time-history pressures at various elevations for both small-size and medium-size dam models. These graphs illustrate a pressure at the dam face resulting from combining the dam excitation effect and the waves generated by the reservoir compressibility. When higher frequency wave effects in the reservoir are excluded, the pressure as a function of time would be a sinusoidal function, with the frequency corresponding to the frequency of excitation. The local peaks in the pressure distribution (Figure 7) are separated by 0.81 seconds, which correspond to the reservoir first natural frequency of 12.18 Hz (period 0.82 second) determined in Equation 8.

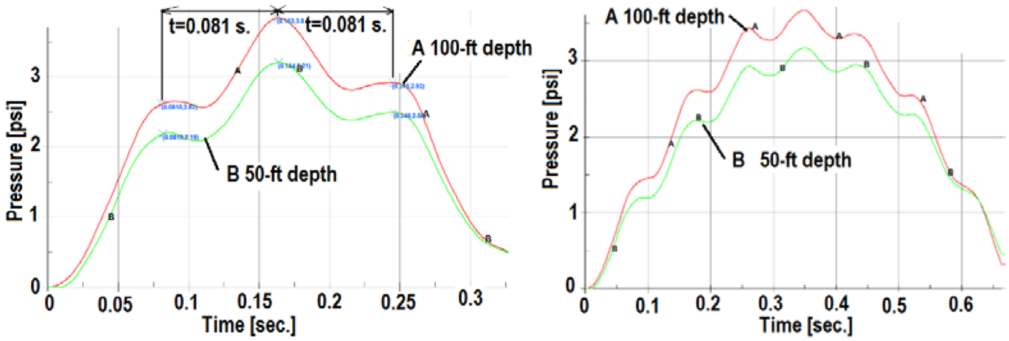

Figure 7. Pressure at the dam face for small size dam with a rigid foundation at 100-foot and 50-foot reservoir depths, for the harmonic excitations at 0.66 seconds (left) and 1.33 seconds (right).

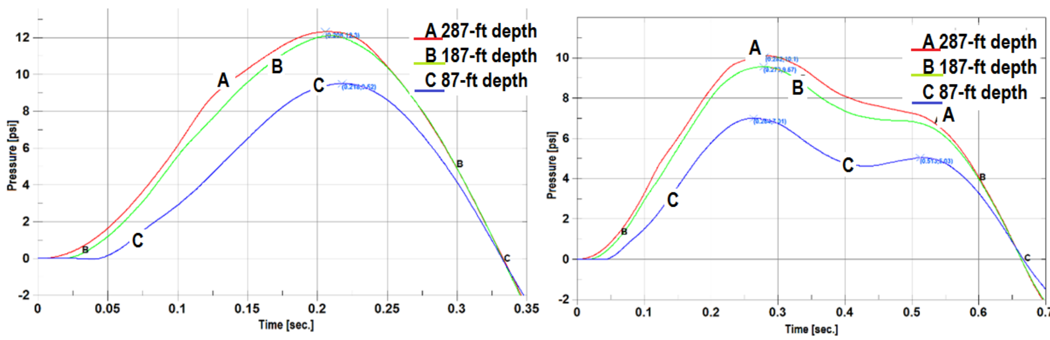

Figure 8. Pressure at the medium size dam face with the rigid foundation at 287-, 187-, and 87-foot depths, for the harmonic excitations at 0.66 seconds (left) and 1.33 seconds (right).

Table 7 shows the comparison of Westergaard's solution and the maximum pressures obtained from the FE analysis for rigid foundation and elastic foundation scenarios, as well as with using various natural periods of excitation.

Table 7. Comparison of maximum pressures at the bottom of the reservoir [lb/in^2]

Reservoir	Foundation and Period	Small Size Dam	Medium Size Dam
Incompressible fluid	rigid	3.43	9.79
Incompressible fluid	elastic	3.76	11.43
Compressible fluid	rigid & (T=0.66 sec.)	3.85	12.3
Compressible fluid	rigid & (T=1.33 sec.)	3.67	10.1
Westergaard approximate solution		3.79	7.58
Westergaard exact solution	T=0.66 sec.	3.25	6.68
	T=1.33 sec.	3.23	6.49

In addition, the FE analysis shows the positive and the negative hydrodynamic pressure turbulence develops in the reservoir during simulation of the dam-reservoir model at the various analysis times (shown in Figure 9 and 10, respectively). Pressure waves that separate from the face of the dam spread along the length of the reservoir until they are absorbed by the “absorbing boundary conditions”, modeled with Perfect Matching Layers (PML) [5].

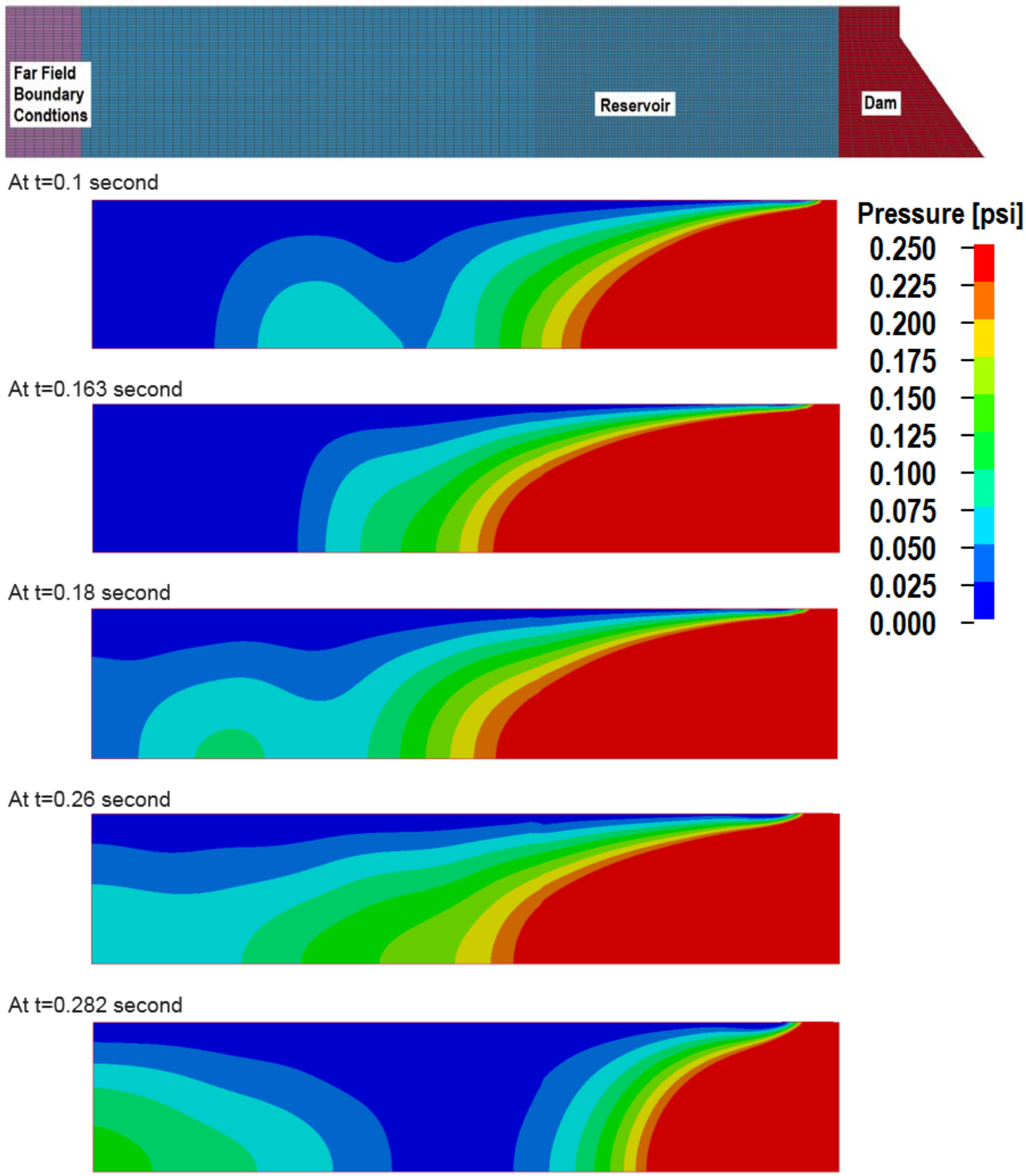

Figure 9. Positive hydrodynamic pressure distribution in the reservoir corresponding to the time line presented in Figure 8 (left).

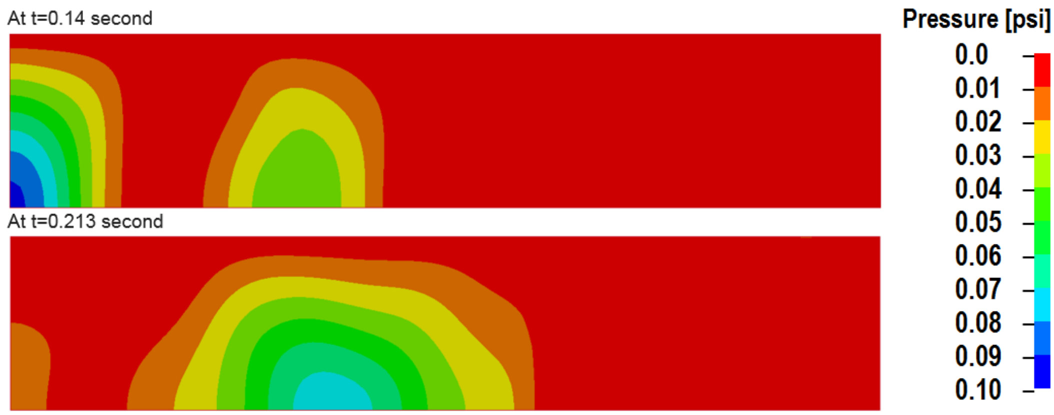

Figure 10. Negative hydrodynamic pressure distribution in the reservoir corresponding to the time line presented in Figure 8 (left).

V. Spillway Radial Gate - Case Study

A. General

A large spillway radial gate structure interacting with the reservoir is analyzed in this section using the approach presented in Section II.

B. FE Model of Radial Gate

A model of a large spillway radial gate structure is analyzed. One half of the gate structure and the corresponding width of the reservoir was analyzed considering symmetry of the model.

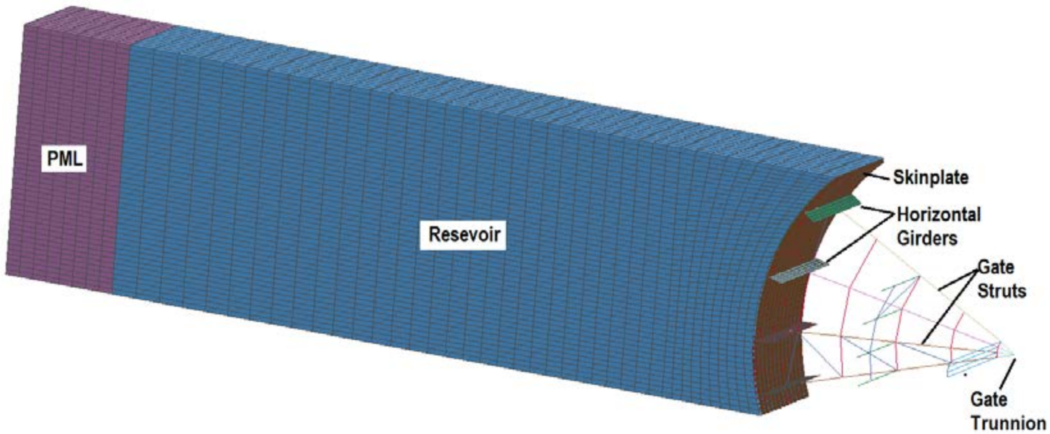

Figure 11. FE model of the radial gate and reservoir (half of the model shown assuming symmetry).

Figure 12 shows the water displacements as the gate moves in the upstream direction during earthquake. Curvature of the gate skinplate allows the free water to “escape” in the upward direction, reducing the hydrodynamic pressure at the upper part of the skinplate. Figure 13 shows the corresponding water pressure distribution (the maximum pressure at the gate bottom edge of 2.04 psi would compare with 1.65 psi and 1.93 psi for Westergaard exact and simplified solutions, respectively.

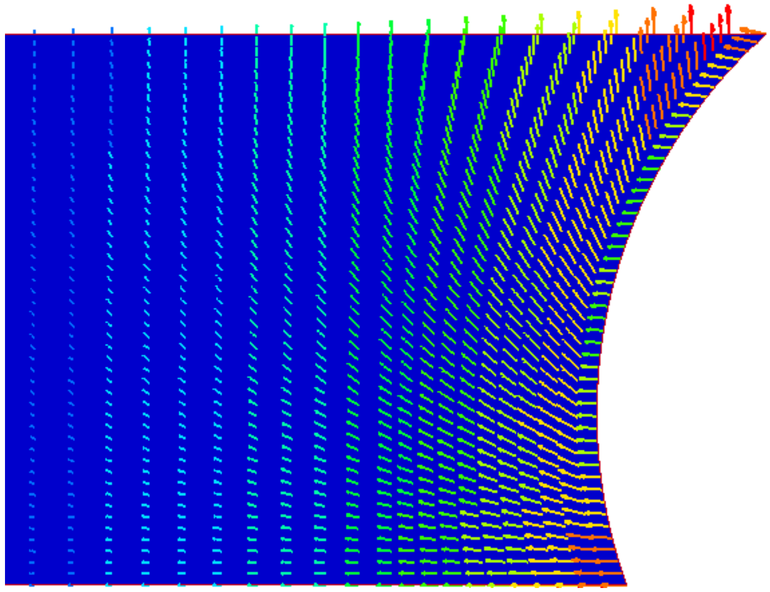

Figure 12a. Total water displacements.

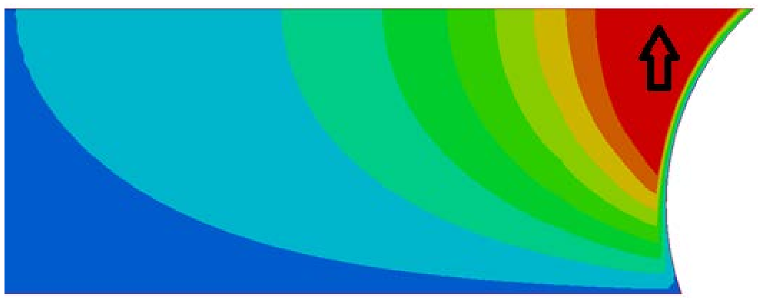

Figure 12b. Horizontal water displacements at gate maximum upstream position (red color - maximum displacement in upward direction).

Figure 13. Water pressure distribution at gate maximum upstream position (corresponding to displacements shown in Figure 12).

Figure 14 shows plots of the trunnion reactions from the FE model compared with the exact and approximate Westergaard's solutions.

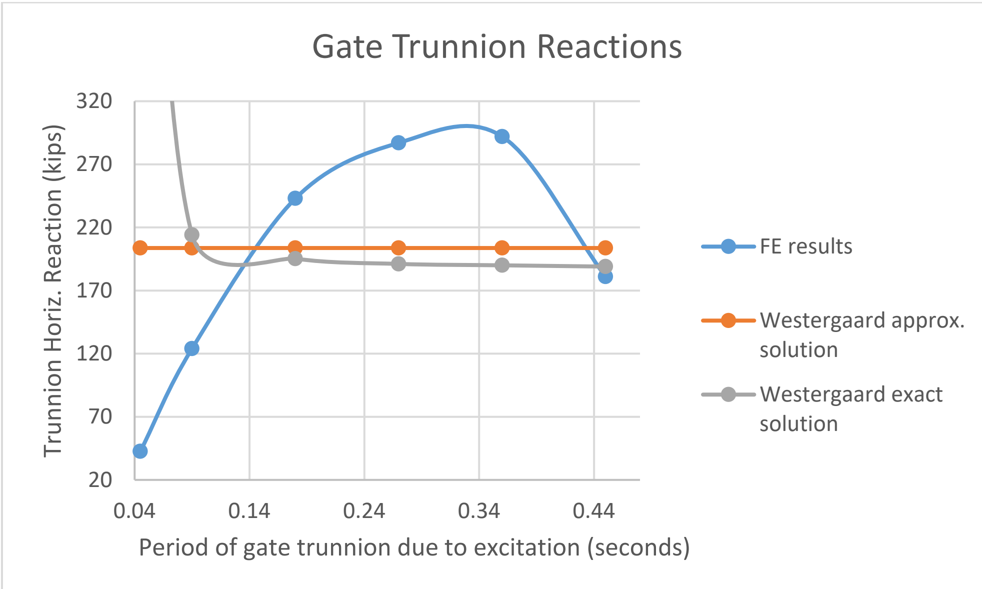

Figure 14. Reaction at the gate trunnion (horizontal) versus periods of trunnion excitations.

The results in Figure 14 show that the hydrodynamic gate trunnion reaction computed in the FE analysis, considering flexibility of the gate structure, is approximately 50 percent higher than the reaction when the Westergaard's "added mass" approach is implemented. This example demonstrated that the seismic analysis of large radial gate structures using the Westergaard approach may significantly underestimate the actual seismically induced hydrodynamic forces in the radial gate structures and the flexibility of the gate structure needs to be considered.

VI. Reservoir-Gate-Dam System

A. General

In this section, a general analysis model of a spillway gate installed at the concrete gravity dam is discussed, as well as aspects of the spillway gate "set-back" effects are evaluated.

It is important to stress again that the determination of hydrodynamic loads on spillway gates induced during earthquakes is a complex process that involves: determination the seismic loads and the response of the dam to these loads; amplification of the accelerations from the base to the dam spillway; and the response of the spillway gates interacting with the reservoir to these seismic loads. Several approaches have been adopted in the past by Reclamation to describe the reservoir-dam and reservoir-spillway gate interaction during an earthquake [11], but there is not one comprehensive method that would provide accurate results without conducting sophisticated numerical analysis. For instance, the approach developed for the seismic design of spillway gates, that is based on the Westergaard added mass approach, would lead in to inaccurate estimations of the hydrodynamic loads on the gate structure, this aforementioned discussion could be found in Section II.B.

Ground accelerations could be significantly amplified during an earthquake from the base of the dam to the spillway. Spillway gates will be subjected to this amplified acceleration, sometimes even several times greater than that measured at the rock abutment. Depending on the response of the dam structure, location of the spillway gate, flexibility of the dam and the gate structure, actual water head on the gate, and whether the transverse, longitudinal or vertical accelerations, the outcome from the analysis may significantly differ.

Simplified methods for computing seismically induced reservoir loads on spillway gates are based on theories developed for concrete dams. In computations of hydrodynamic loads on dams and gates, an approximate method developed by Westergaard is often used. These solutions do not account however for the flexibility of the dam nor the gate structure, amplifications of the ground motion acceleration up through the dam, the three-dimensional effects, actual geometry of the gate skinplate, or the position of gates with respect to the face of the dam and can lead to imprecise results.

Dynamic stability analyses of spillway gates performed with the simplified methods could grossly miscalculate hydrodynamic loads on the gate structure. The result could be costly, where potentially unnecessary modifications to existing gates, over-design of new gates, or unreliable risk assessments based on inaccurate analyses of the gates may be considered.

B. Spillway Gate Set-back Effect

In Section V, we covered the discussion of amplified hydrodynamic effect on a radial gate, when a significant controlling factor is the gate curvature and the flexibility of the structure. In contrast, there exists a scenario when the total pressure acting on the gate reduces as the gate location is “set-back” away from the dam face. This section briefly describes results of an investigation of the gate “set-back” effect conducted in [7] to illustrate sensitivity of the analysis results to various considered parameters. The results of the FE analysis are supported by the experimental data [8] (NOI curve in Figure 18) which showed that the spillway gates experience significantly lower hydrodynamic loads from the reservoir during earthquakes when the gates are set back from the upstream face of the dam. As an effect of this study, an empirical formula was developed in this study, that bases on the exact Westergaard solutions. Equation 30 provides an approximation calculating the pressure over the face of the vertical gate that is “set-back” from the face of the dam by a ratio β. Both the effect of the gate height and the set-back distance were incorporated in Eq. 30 and illustrated in Figure 15.

$$P_{Total}(h) = P_{Westergaard} \cdot (1.1 - 0.45\beta) \qquad (\beta \leqq 0.7) \qquad \text{Eq. 30}$$

where:
$\beta = d / h_1$ is the gate set-back ratio defined as a distance of the gate location to the face of the dam divided the gate height (Figure 15)
$P_{Westergaard}$ = is the pressure distribution determined from the exact Westergaard solution, Eq.5.

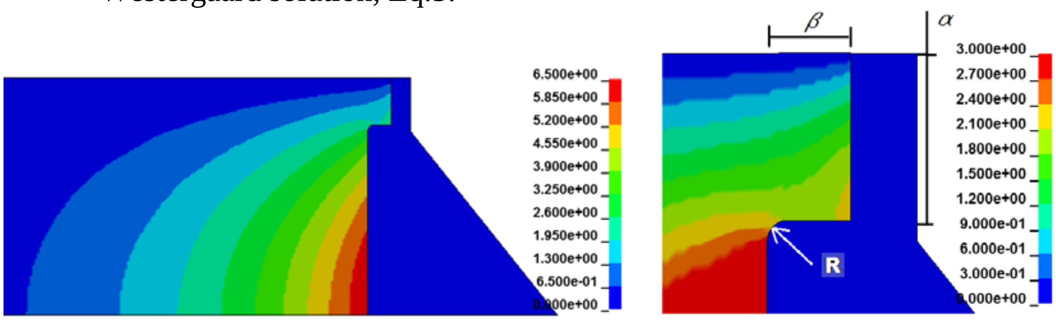

Figure 15. Hydrodynamic pressure [psi] for 200-feet deep reservoir with height h_1=50 feet, β=0.5 and ground acceleration of 0.1g.

Figure 16 shows the total load on the gate versus the ratio of the distance of gate location to the face of the dam and the gate height, β.

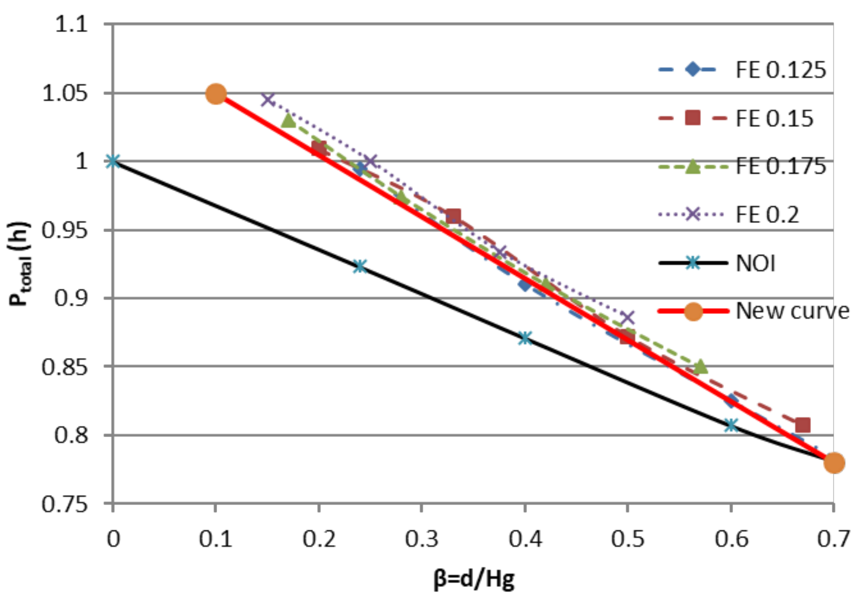

Figure 16. A proposed relation (New curve) developed to account for the "set-back" effect in calculation of total hydrodynamic load on vertical gates.

In the presented study, a formula was developed to determine seismically induced hydrodynamic loads on vertical spillway gates installed at the rigid dam with the vertical upstream face. The approach is based on the exact Westergaard's solution with the vertical gate set back from the dam face. The study shows that pressure reduction is observed as the crest spillway gate is set back from the face of the gravity dam.

C. Comprehensive Analysis of the Gate–Dam-Reservoir System

General

As referenced in Section VI.B, the solution for the gate "set-back" effect illustrates how important it is to consider various factors in the seismic analysis of the spillway gates. The differences in the computed loads on the gate could be significant when flexibility of the dam and spillway gate structure, and the actual geometry of the gate, or its position with respect to the face of the dam are considered.

Global Approach

For large spillway gates installed at large concrete dams, all the factors listed in the General section, above, may significantly influence the actual hydrodynamic loads during large earthquakes. Consideration for all these aspects in one large FE model may not be practical based on the current development stage of the FE software as long computation time may be required. A more practical approach would involve an analysis conducted in the stage phases as described below.

Since the dominating seismic loads for gravity dams and spillway gates are in the upstream/downstream direction, the large three-dimensional FE model could be reduced considering a single gate (or a half of it, if a symmetry assumption applies) together with the corresponding width of the dam monolith, the reservoir, and the foundation (Figure 17).

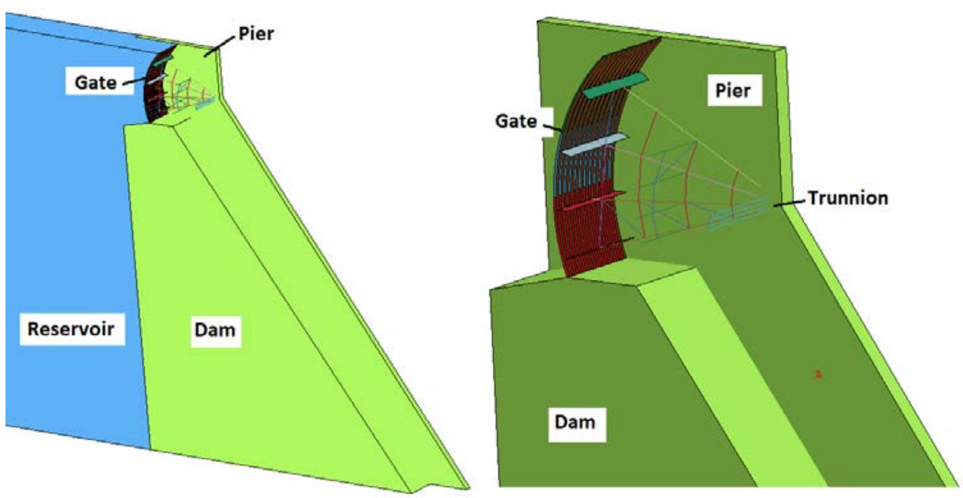

Figure 17. A model of the radial gate-dam monolith-reservoir (left) and a closed view of the spillway (right); a half of the model shown.

The model in Figure 17 allows precise computations of the hydrodynamic loads on the spillway gate. It includes the actual geometries of the gate, the spillway, and the dam; incorporates the amplification of acceleration over the height of the dam monolith; incorporates the interaction between the reservoir and the gate; and flexibility of the gate structure and the gate "set-back" effect. The size of the FE model appears to be reasonable. If the size of the model cannot be accommodated by the software however, the following simplified procedure is proposed:

1) First, a seismic analysis of the single dam monolith-reservoir-foundation system with a simplified model of the spillway gate is conducted. Accelerations at the spillway: for radial gates at the trunnion locations, but for other gates at the gate supports are recorded and are used as an input for a "separated" detail gate structure model.
2) Then, a separate analysis of the detail gate-reservoir system is performed using, the computed accelerations from the dam monolith-reservoir-foundation model.

Both approaches are currently being evaluated by the author of this report. The initial investigation results are promising and as the studies are completed, an approach will be proposed for the Dam Safety evaluations of the concrete dams and the spillway gates.

VII. Conclusions

A. Summary

In the report and the accompanied USSD conference papers (included in the Appendix), three methods are presented and evaluated, which are commonly used in the time analysis of the dam-reservoir-foundation systems for earthquake loads. These include: the "added mass" approach, the "acoustic fluid", and the "fluid-like material model" methods. The theory for each of the methods is presented and it is illustrated by the results for a case of two concrete dams: a small size dam and a medium size dam.

B. Conclusions

The following conclusions could be formulated based on the results of the investigations:

- The differing results of the blind predictions in the Monticello Dam analysis appear to be primarily due to the various approaches selected by participants for modelling fluid-structure interaction. Of the three approaches, the "added mass" approach offers the least confidence for accuracy of the solution.
- The "added mass" approach, based on the approximate Westergaard's solution, roughly estimates the mass of water interacting with the dam during an earthquake. The error is particularly large when the excitation

frequency is similar to the first natural frequency of the reservoir. Even greater errors would exist in Westergaard's solutions if the dam face was not vertical, or if the dam and the foundation are considered not rigid.

- Estimations of an added mass from Westergaard's formulas assumes a constant mass of the water that is forced to move with the dam during the ground motion. In the true time behavior of the dam-reservoir system, the mass of water varies as the dam displaces and deforms, which leads to a varying volume of water interacting with the dam during an earthquake. Therefore, the "added mass" approach should not be implemented in any time-history analysis for fluid-structure interaction problems. Its use should be limited to a preliminary estimation of seismically induced hydrodynamic loads on dams.
- Compressibility of water is an important factor that influences the hydrodynamic pressure distribution in the reservoir. The time analysis with an "incompressible fluid" material model provides significantly different results when compressibility of the fluid is considered.

C. Future Research

The following are the recommended future research topics related to hydrodynamic interactions between the reservoir, dam, and spillway gate structures:

- Calibration of the FE analysis with the laboratory test results
    - Plan: Ongoing laboratory testing (conducted in the Reclamation's Hydraulic Laboratory of a 4-foot by 4-foot structure installed in a water flume), is expected to be a primary benchmark test to be used in the calibration of the FE models.
    - Implement and evaluate a hybrid frequency-time domain analysis approach the seismic simulations of the dam-reservoir-foundation system [6].
    - Investigate the sensitivities of water viscosity parameters in the numerical analysis of a dam-reservoir interaction problems.
- "A priori" and "a posteriori" error estimations of the numerical solutions [9] [10].
    - Plan: Reclamation' Technical Service Center is involved in evaluations of accuracy of numerical solutions for advanced mathematical models describing an interaction of the reservoir-dam-gate system. Some of these initiatives include publications:
-

    1. Publishing conference papers on the subject [6], [7], [12].
    2. Involvement in organizing USSD Workshops on *Seismic Analysis of Concrete Dams* in 2017 and *Evaluation of Numerical Models and Input Parameters in the Analysis of Concrete Dams in 2018.*
    3. TSC interaction with the international engineering community and contribution to developments of new technical reports [13].

IX. References

[1] Bureau of Reclamation, DSO-2018-09 report, Guide for Analysis of Concrete Dam Structures using Finite Element Methods, March 2018

[2] Westergaard H. M., "Water Pressures on Dam during Earthquakes," *American Society of Civil Engineers,* Vol. 98, o. 2, pp. 418-433, 1933

[3] Zanger C. N., *Hydrodynamic pressures on Dams due to horizontal Earthquake Effects*, Bureau of Reclamation, Engineering Monograph No.11., 1952

[4] Manie J. (Ed.), DIANA User's Manual, Delft, 2017

[5] Livermore Software Technology Corporation, LS-DYNA -Version 971

[6] Salamon J., *Numerical Assessment of Hydrodynamic Loads Induced during Seismic Interaction between Reservoir and Concrete Dam*, USSD Conference, Anaheim, 2017

[7] Salamon J., *Evaluating Seismically Induced Hydrodynamic Loads on Spillway Gates*, USSD Conference, Louisville, 2015

[8] Nakayama Y., Ohmachi T., Inoue S. (1991), *Practical Evaluation of Hydrodynamic Pressures on Dam-Gates during Earthquake*, Proceeding of JSCE A, Vol. 64, No.4, pp. 959-969, 2008. (in Japanese).

[9] Bathe K.-J., "Finite Element Procedures in Engineering Analysis," Prentice-Hall, Inc., Englewood Cliffs, 1982

[10] Gratsch T.and Bath K.-J., "A posteriori error estimation techniques in practical finite element analysis," ELSERVIER Computers & Structures Journal, 2004.

[11] Salamon J., *Seismic Induced Loads on Spillway Gates – Phase 1 – Literature Review*, Bureau of Reclamation, Report DSO-11-06, 2011.

[12] Salamon J., Proceedings for the 14th ICOLD International Benchmark Workshop on Numerical Analysis of Dams, Stockholm, 2018

[13] Salamon J., et al., *Design of Lock Gates under Seismic Action,* PIANC, The World Association for Waterborne Transport Infrastructure, Report No. 151, 2016

X. Appendix

In this Appendix, conference publications are attached that were prepared as a part of this research sponsored by this Reclamation's Dam Safety Technology Development Program.

EVALUATING SEISMICALLY INDUCED HYDRODYNAMIC LOADS ON SPILLWAY GATES

Jerzy Salamon PE, PhD[1]

ABSTRACT

The determination of seismically induced hydrodynamic loads on spillway gates is a complex process that involves the seismic response of the dam, the response of the spillway gates, and the response of the reservoir. Several research studies have been conducted to determine the reservoir-dam and reservoir-spillway gate interaction during an earthquake, but there is not a comprehensive method that would provide satisfactory and accurate results without conducting sophisticated numerical analysis.

As a background, the dynamic reservoir loads developed during an earthquake are of importance in the design and evaluation of the spillway gates. The ground acceleration at the base of a dam during an earthquake can be considerably amplified at the top of the dam. Spillway gates will be subjected to this amplified acceleration, sometimes several times greater than that measured on rock at the abutment, depending on the response of the dam structure, location of the spillway gate, flexibility of the dam and the gate structure, actual water head on the gate, and whether the transverse, longitudinal or vertical acceleration is considered.

Dynamic stability analyses of spillway gates performed with the simplified methods could grossly miscalculate hydrodynamic loads on the gate structure. The result could be costly, where potentially unnecessary modifications to existing gates, over-design of new gates, or unreliable risk assessments based on inaccurate analyses of the gates are performed.

Standard methods for computing seismically induced reservoir loads on spillway gates are based on theories developed for concrete dams. In particular, the typical practice for computing hydrodynamic loads on dams relies on an analytical method developed by Westergaard. These solutions do not account for the flexibility of the dam nor the gate structure, amplifications of the ground motion acceleration up through the dam, the three dimensional effects, actual geometry of the gate skinplate, or the position of gates with respect to the face of the dam.

This paper presents the results of numerical analyses for rigid dams interacting with the reservoir, compares the results with the classical Westergaard solutions, and evaluates the spillway gate set back effect on the hydrodynamic loads induced during earthquakes.

[1]Technical Specialist, Waterways & Concrete Dams Group, Bureau of Reclamation, P.O. Box 25007, Denver, Colorado, 80225, USA, e-mail: jsalamon@usbr.gov

INTRODUCTION

Spillway gate structures in the closed position are exposed to a variety of loads including dead loads, hydrostatic pressure, seismic loads, ice loads, wave's effects from the reservoir and earthquake induced hydrodynamic reservoir loads. Some other loads are developed during gate operations.

Several research studies have been conducted to determine the reservoir-dam interaction during earthquakes but there is not a comprehensive method that would provide satisfactory and accurate results of hydrodynamic loads on spillway gates during seismic events. An overview of the analytical analysis methods used to determine hydrodynamic loads on dams and spillway gates was performed by Salamon (2011). A brief summary of the selected methods is provided below.

Hydrodynamic Loads on Dams

The first systematic analysis of the dam-reservoir interaction was performed by Westergaard (1931) in connection with the design of Hoover Dam by the Bureau of Reclamation (Reclamation). In the study of the earthquake response of a rigid dam with vertical upstream face, Westergaard developed an analytical solution for the hydrodynamic pressure distribution as a result of a harmonic horizontal motion of the dam. The approximate formula for the parabolic hydrodynamic pressure distribution over a vertical dam face, presented in a fundamental and simplistic form, has been used continuously by the industry in the analysis and design of concrete dams.

Zangar (1952) of Reclamation estimated experimentally the hydrodynamic pressures at the inclined upstream face of rigid dams using the electric analogy tray and then developed empirical formulas for various shapes of the dam upstream face.

Housner (1954) derived and solved an equation for fluid containers under earthquake loading incorporating a length of the reservoir in the formula. Housner made a distinction between an impulsive pressure that relates to the portion of the fluid that moves in coherence with the structure (the added mass), and the convective pressure that relates to effects like sloshing. Solutions for a rectangular, trapezoidal, segment, and stepped dam were provided as well as for flexible retaining walls.

Chwang (1978) and Chwang & Housner (1978) developed an analytical solution of seismic induced hydrodynamic forces for a rigid dam with an inclined upstream face of constant slope by potential-flow theory and momentum method, adopting von Karman's (1931) momentum-balance approach.

Effect of pressure wave absorption by sediment at the bottom of the reservoir was investigated by Chopra and Fenves (1983). The research results demonstrated that sediment in reservoirs plays an important role in assessing the real hydrodynamic reservoir pressure on the dam.

An extensive study was conducted at the University of California at Berkeley for earthquake analysis of concrete dams. The wave equation governing the motion of water in a reservoir was solved in the frequency domain using numerical methods and the solution was implemented in computer programs EAGD by Chopra (1983) and EADAP by Ghanaat (1989).

Lee and Tsai (1991) developed a closed-form solution for the analysis of the dam-reservoir system in the time domain. Studies were performed for the dam when the reservoir was both empty and full, considering the interaction between the fluid and the structure. The results of the investigation demonstrated that compressibility of the fluid and flexibility of the dam structure had greatest impact on interactive forces to both the structure and reservoir.

Several analyses were performed on a coupled dam-reservoir system composed of elastic and non-elastic dam material with compressible water, structural damping of the dam material and radiation damping of the water using numerical methods.

Hydrodynamic Loads on Spillway Gates

An experimental and Finite Element (FE) study was performed by Nakayama et al. (1991) for crest spillway gates set back from the vertical face of a rigid dam. As a result of the study, an analytical method was formulated for estimation of the seismic induced hydrodynamic loads on vertical spillway gates based on the simplified Westergaard solution.

Hydrodynamic loads on Folsom Dam spillway radial gates were analyzed by Reclamation. A methodology for determining the seismic induced hydrodynamic loads on spillway gates was summarized by Todd (2002). In the approach, a pseudo-static earthquake load was determined by including the effect of the “water added-mass” (reduced for a curved radial gate skinplate shape) and the earthquake related magnification factor for the dam.

Sasaki, Iwashita and Yamaguchi (2007) studied the basic characteristics of hydrodynamic pressure acting on spillway gates during an earthquake based on numerical analysis that considered vibrations of the dam body and the gate. They proposed a method for calculating hydrodynamic pressure during an earthquake in the seismic analysis of gates.

Versluis (2010) performed an extensive study on the hydrodynamic loads on large lock gates at the Technical University in Delft. This research was related to the design of the rolling gates for the new Panama Canal Locks. The Westergaard and Housner methods were implemented. Versluis concluded that the Housner formula for calculating hydrodynamic loads on the gates is more appropriate for the lock structure when the length of the reservoir is comparable with its depth. In the research a contribution of sloshing effects on the gates was also investigated.

PROBLEM STATEMENT FOR INTERACTION BETWEEN RESERVOIR AND SPILLWAY GATE

Analytical solutions obtained by Westergaard, Chwang, Housner, and others for a regular shape of the dam face would be impossible to derive for an irregular geometry of a dam with installed spillway gates. However, numerical methods can be used to solve the system of governing equations for the dam/gate system with complex boundary conditions. For the dam-gate-reservoir model shown in Figure 1, the problem for seismic induced motions can be formulated in a form of the Boundary Value Problem using Equations 1 through 5 below.

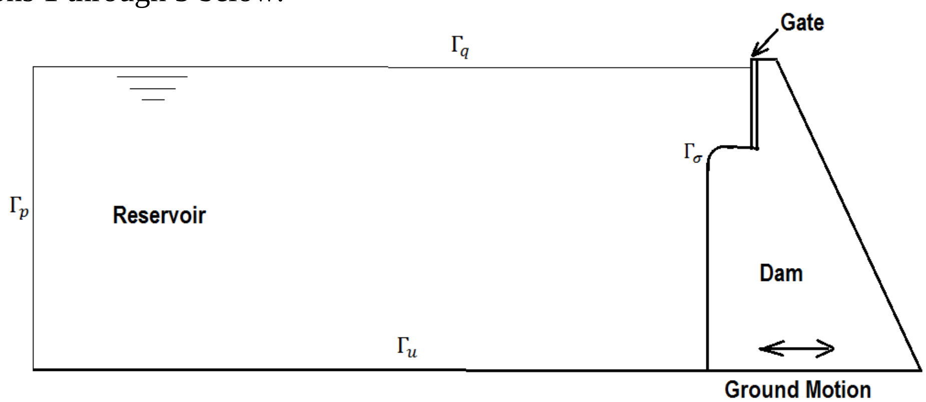

Figure 1. Model of the Dam-Gate-Reservoir System.

Problem Statement for Dam-Gate-Reservoir System

In the continuum theory of mechanics, the set of basic equations that includes equations of motions (Eq.1), geometric equations (Eq.2), and material constitutive law (Eq.3), together with boundary and initial conditions (Eq.4 and Eq.5), defines a mathematical formulation of the dynamic problem for linear elastic materials for fluid and concrete structure.

Equations of Motions. $\sigma_{ij,j} + \rho b_i = \rho \ddot{u}_i \qquad i,j,k = 1,2,3$ (Eq.1)

Geometric Equation. $\varepsilon_{ij} = \frac{1}{2}\left(u_{i,j} + u_{j,i} + u_{k,i}u_{k,j}\right)$ (Eq.2)

Constitutive Law for the Dam. $\sigma_{ij} = \frac{E}{1+\nu}\left(\varepsilon_{ij} + \frac{\nu}{1-2\nu}\varepsilon_{kk}\delta_{ij}\right)$ (Eq.3)

Constitutive Law for the Reservoir. $p = \frac{1}{3}\sigma_{kk} = K\,\varepsilon_{kk}$

where: $\underline{u}$, $\underline{\varepsilon}$, $\underline{\sigma}$, p are displacement, strain, stress tensors, and pressure
ρ, b, are mass density and body force
E, ν, K are elastic modulus and Poisson ratio of concrete, and bulk modulus of fluid.

Boundary Conditions.

$$\sigma_{ij} n_j = T_i \qquad on\ \Gamma_\sigma$$

$$\bar{q} = 0 \qquad on\ \Gamma_q$$

$$u_i = 0 \qquad on\ \Gamma_u \qquad \text{(Eq.4)}$$

$$p = \bar{p} \qquad on\ \Gamma_p$$

Γ_σ, Γ_q, Γ_u, Γ_p are parts of the boundary shown in Figure 1.

Initial Conditions.

$$u_i(x, t_0) = u_i^0(x) \qquad \dot{u}_i(x, t_0) = v_i^0(x) \qquad \ddot{u}_i(x, t_0) = a_i^0(x) \qquad \text{(Eq.5)}$$

Solution. Applying the standard procedure for derivation of the virtual power principle and considering geometric relationships between the displacements and strains, constitutive equations, and the initial conditions, the finite element discretization of the Galerkin variational formulation of the preceding equations results in the following system of second order differential equations:

$$\mathbf{M}_S \ddot{\mathbf{U}} + \mathbf{C}_S \dot{\mathbf{U}} + \mathbf{K}_S \mathbf{U} = \mathbf{F}_g + \mathbf{F}_p \qquad \text{(Eq.6)}$$

where: $\mathbf{M}_s$, $\mathbf{C}_s$, and $\mathbf{K}_s$, are the mass, damping and stiffness matrices, respectively

The unknown vector of nodal variable **U** represents the relative displacements at the nodes of the FE model of the dam. The forcing vector $\mathbf{F}_g = \mathbf{M}_s \ddot{\mathbf{U}}_g$ contains forces generated by the ground acceleration applied to the dam nodes. The vector $\mathbf{F}_p$ represents the hydrodynamic forces acting on the upstream face of the dam and it is related to the unknown vector of nodal pressures. To solve the problem in the time domain, an explicit approach has been implemented.

WESTERGAARD'S SOLUTIONS

Description of Westergaard's Approach

Exact Solution. The seismic motion of a straight rigid concrete gravity dam of height *h* with an infinite reservoir length, shown in Figure 1, was mathematically expressed by Westergaard in terms of the theory of elasticity of solids based on the formulation provided by Lamb (1924). Two equations of motion, a linear kinematic relation for small deformations, and an elastic constitutive equation without shearing stresses, together with the boundary conditions (stresses equal zero on the reservoir surface, vertical displacement equal zero at the bottom of the reservoir) described the two-dimensional physical model of the dam-reservoir system. The solution of the problem with horizontal and vertical motions of the water (plane strain) was given by Westergaard in the form of a stress (pressure) distribution in the reservoir by Eq.7.

$$\sigma = -\frac{8\alpha w h}{\pi^2}\cos\frac{2\pi t}{T}\sum_{1,3,5,\ldots}^{n}\frac{1}{n^2 c_n}e^{-q_n}\sin\frac{n\pi y}{2h} \tag{Eq.7}$$

$$q_n = \frac{n\pi c_n x}{2h} \quad c_n = \sqrt{1-\frac{16 w h^2}{n^2 g k T^2}}$$

According to Eq. 7, the maximum pressure *p* occurs when the dam is in the extreme positions (t = 0, T, 2T, etc.) during motion, so the maximum water pressure distribution at the upstream face of dam (for x =0, $q_n = 0$) could be expressed by Eq.8.

$$p = \frac{8\alpha w h}{\pi^2}\sum_{1,3,5,\ldots}^{n}\frac{1}{n^2 c_n}\sin\frac{n\pi y}{2h} \tag{Eq.8}$$

$$c_n = \sqrt{1-\frac{16 w h^2}{n^2 g k T^2}} = \sqrt{1-\frac{0.71889}{n^2}\left(\frac{h\ \text{sec.}}{1\,000\ T\ \text{ft.}}\right)^2}$$

where: *x*, *y* = the axis of *x* is at the surface of the water directed upstream and the axis *y* is vertical downward (Figure 2),

w = weight of water per unit volume (*w* = 62.4 lb/ft^3),

g = acceleration due to gravity (*g* = 32.2 ft/sec^2)

α = maximum horizontal acceleration of foundation divided by *g*,

T = period of horizontal vibration of the foundation,

t = time,

k = bulk modulus of water (*k* = 300,000 lb/ft^2)

The solution expressed by Eq.7 and 8 was derived with the following assumptions:

- The dam upstream face is straight and vertical,
- The dam does not deform and is considered to be a rigid block,
- The reservoir is infinite in length,
- Dam sinusoidal oscillations are horizontal,
- Small motions are assumed during earthquake,
- The problem is defined in 2-D space,
- Period of free vibration of the dam, T_0, is significantly smaller than the period of vibration, *T*, of the earthquake (resonance is not expected),
- Non-dimensional horizontal acceleration of $\alpha = 0.1$,

The effect of water compressibility was found to be small in the range of the frequencies that are supposed to occur in the oscillations due to earthquake.

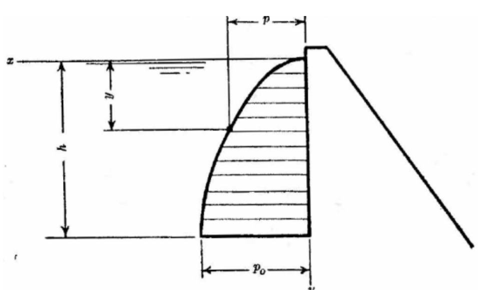

Figure 2. Pressure distribution on dam for the Westergaard's exact solution.

Approximate Solution. The hydrodynamic water pressure on the dam expressed by Eq. 8 was simplified by a parabola described by Eq. 9.

$$p = 0.875\, w\, \alpha\ (h\, y)^{0.5} \qquad \text{(Eq.9)}$$

This approximate Westergaard's formula (Eq. 9) is widely used by the industry in the preliminary calculations of the hydrodynamic pressure on dams.

Hydrodynamic Loads on Vertical Face of Rigid Dam

In this section Westergaard's approximate and exact solutions are compared with the FE analysis solution. For the purpose of this study a spreadsheet was developed to calculate the pressure distribution at the face of the dam for both Westergaard's formulas. The spreadsheet was calibrated with the results derived by Westergaard (1931). Figure 3 presents hydrodynamic pressure distribution for the reservoir depths of 200, 400, and 600 feet with the period of horizontal dam vibrations, T, between 0.33 and 4 seconds.

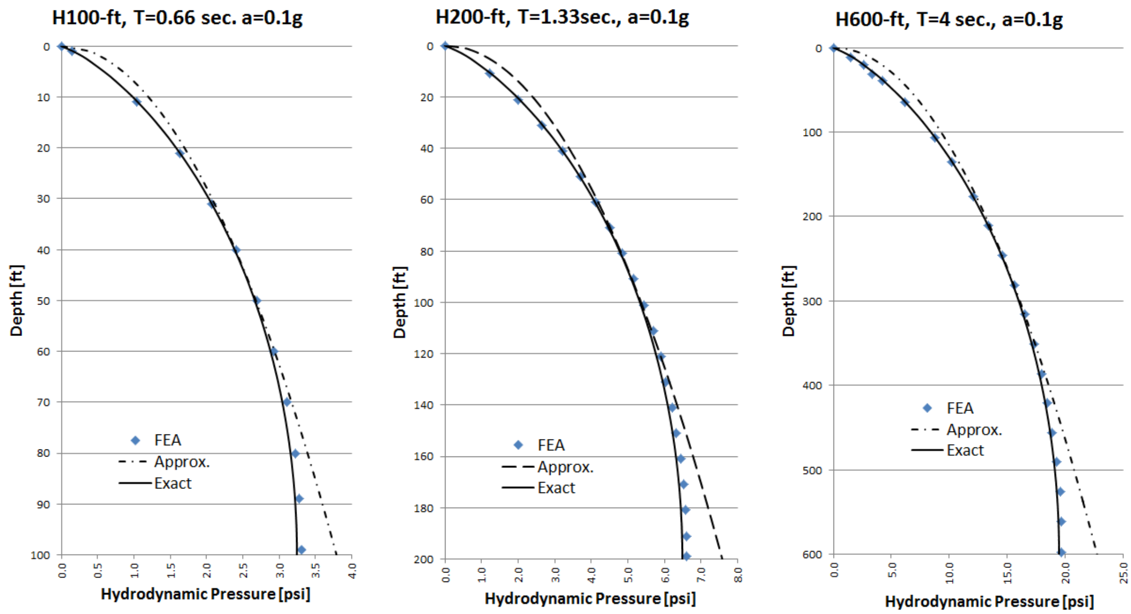

Figure 3. Comparison of hydrodynamic pressures calculated according to Westergaard's exact and approximate formulas and the FE results for ground acceleration of 0.1g.

Good agreement between the exact Westergaard's solution and the FE results for a rigid dam with vertical upstream face can be observed in Figure 3. In general the approximate Westergaard's formula (Eq.9) overestimates the hydrodynamic pressure at the upper part of a rigid dam when it is compared with the exact Westergaard's solution and the FE analysis results.

HYDRODYNAMIC LOADS ON SPILLWAY GATES

Seismically induced hydrodynamic pressure from the reservoir during an earthquake acts on the spillway gates in the same way it acts on the dam body. In this section, a basic study is performed to investigate the effect of the gate set back from the dam face. A FE analyses is performed for a rigid dam with vertical upstream face and the spillway gate located at various distances from the upstream face of the dam. Finally, an analytical method is proposed for estimation of the hydrodynamic loads on vertical spillway gates when the gates are set back from the dam face.

Gate Set-back Effect

Nakayama et al. (2007) performed an experimental study to determine hydrodynamic loads on spillway gates installed at a rigid dam with vertical upstream face. The results of the experiments supported by the FE analysis showed that during earthquakes, the spillway gates experience significantly lower loads from the reservoir when the gates are set back from the upstream face of the dam. They developed an empirical formula (Eq. 10) for the pressure distribution over the vertical face of the spillway gate based on the FE analysis results. The effect of the gate height and the set-back distance (Eq. 11 and Eq. 12) was incorporated in the study.

$$p_g(h) = p_{FEM,\beta=0}(h) \cdot C(h) \qquad \text{(Eq.10)}$$

$$C(h) = 1 - \frac{\beta h}{2h_1} \qquad (\alpha \leqq 0.3, \beta \leqq 0.7) \qquad \text{(Eq.11)}$$

$$C(h) = (1-\sqrt{\alpha})\exp\left(\frac{-1.4\beta h}{h_1}\right) + \sqrt{\alpha} \qquad \text{(Eq.12)}$$

where:
α is the ratio of the depth of the gate to the reservoir depth = h_1 / H
$\beta = d / h_1$ is the gate set-back ratio defined as a distance of the gate location to the face of the dam divided the gate height

Nakayama et al. developed also a simplified formula (Eq. 13) for the total hydrodynamic load on spillway gates that was based on the approximate Westergaard's solution (Eq.9).

$$P_g = {}^{7}/_{12}\, k\, w\, \sqrt{H}\ \ h_1^{1.5}\ \left(1 - {}^{3\beta}/_{10}\right) \qquad \alpha \leqq 0.3,\ \ \beta \leqq 0.7 \qquad \text{(Eq.13)}$$

FE ANALYSIS

For a cross-section of the spillway typical for Reclamation's gravity dams, a FE analysis was performed for a rigid dam with various gate heights (α), various gate set back distances (β) and a 5-foot-radius of the spillway approach channel (Figure 4). Distribution of the hydrodynamic pressure in the 200-foot-deep reservoir is shown in Figure 4 for the gate to dam height ratio of 0.2, the ratio of the gate set back distance to the gate height of 0.5, and for ground acceleration of 0.1g.

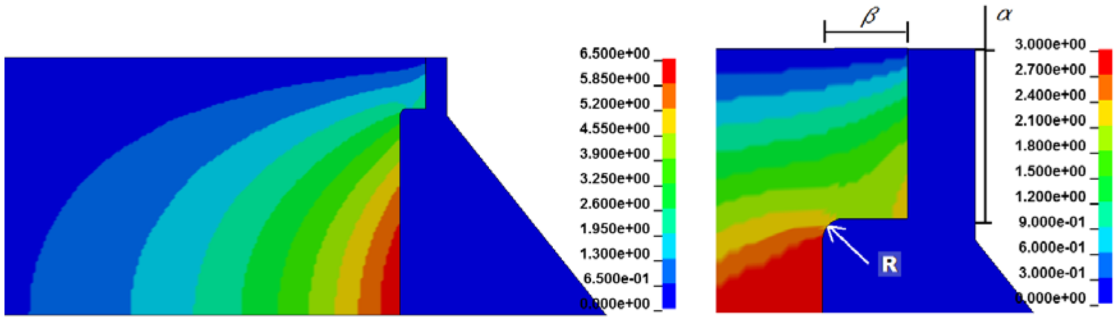

Figure 4. Hydrodynamic pressure [psi] for 200-feet deep reservoir with α=0.2, β=0.5 and ground acceleration of 0.1g.

<u>Nakayama's Solutions vs FE Results</u>

In this section, the solution proposed by Nakayama et al. (NOI) by Eq. 10 is compared with the FE analysis results obtained for the model shown in Figure 4.

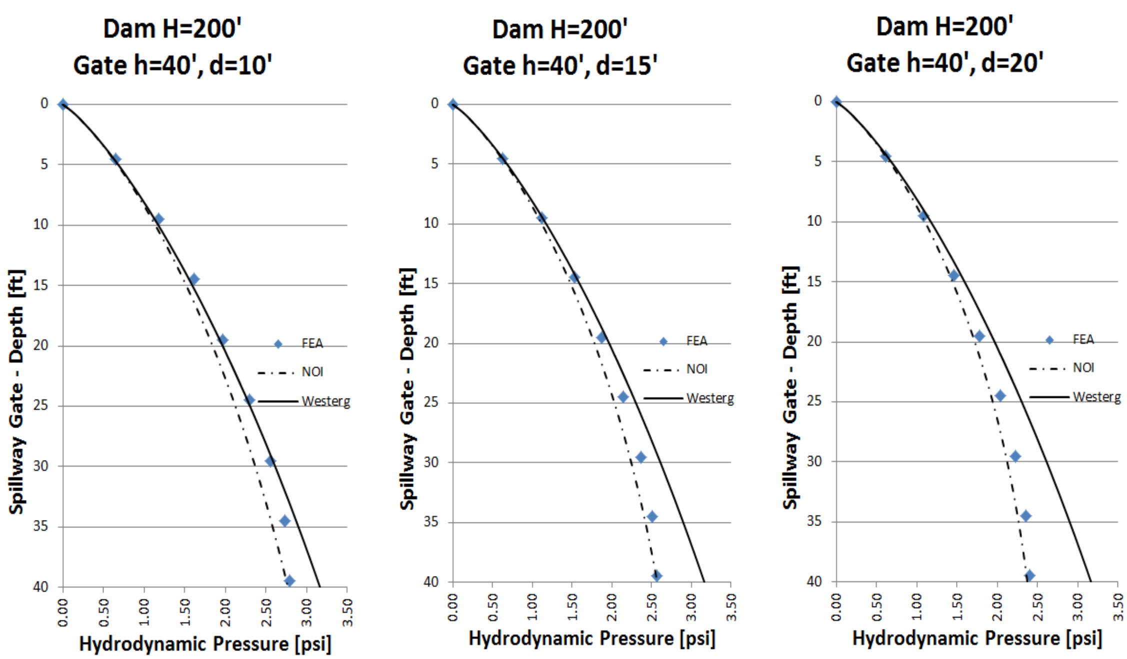

Figure 5. Comparison of hydrodynamic pressures [psi] for the gate set back distance at 10-, 15-, and 20-feet (β=0.25, 0.375, and 0.5, respectively), the 40-ft high spillway gate, 200-feet deep reservoir (α=0.2) and ground acceleration of 0.1g.

According to Figure 5, the hydrodynamic pressure on the gate decreases as the gate set back distance from the dam face increases. Nakayama et al. (NOI) solution shows lower pressure on the gate when compared with the FE analysis results.

HYDRODYNAMC LOADS ON SPILLWAY GATES BASED ON WESTERGAARD'S EXACT SOLUTION

A new approach for calculating hydrodynamic loads on spillway gates is proposed in this paper. The approach is based on the Westergaard's exact solution (Eq.7), and is calibrated with the FE analysis results performed for various gate heights and gate set-back distances and using Nakayama et al. equations (Eq. 10 and Eq. 11). The main advantage of the proposed method is simplicity and the fact that it does not require FE analysis of the dam to determine loads on vertical spillway gates.

For rigid dams with a vertical face, the total load on the vertical gates computed in the FE analysis is presented in Figure 6 as a function of the gate set back distance to gate height ratio. The Figure shows also the "New Curve" (Eq. 14) that is an approximation of the FE analysis results and the curve "NOI" developed by Nakayama et al. The new equation for the total hydrodynamic load on a vertical gate is:

$$P_{Total}(h) = P_{Westergaard} \cdot (1.1 - 0.45\beta) \qquad (\beta \leqq 0.7) \qquad \text{(Eq.14)}$$

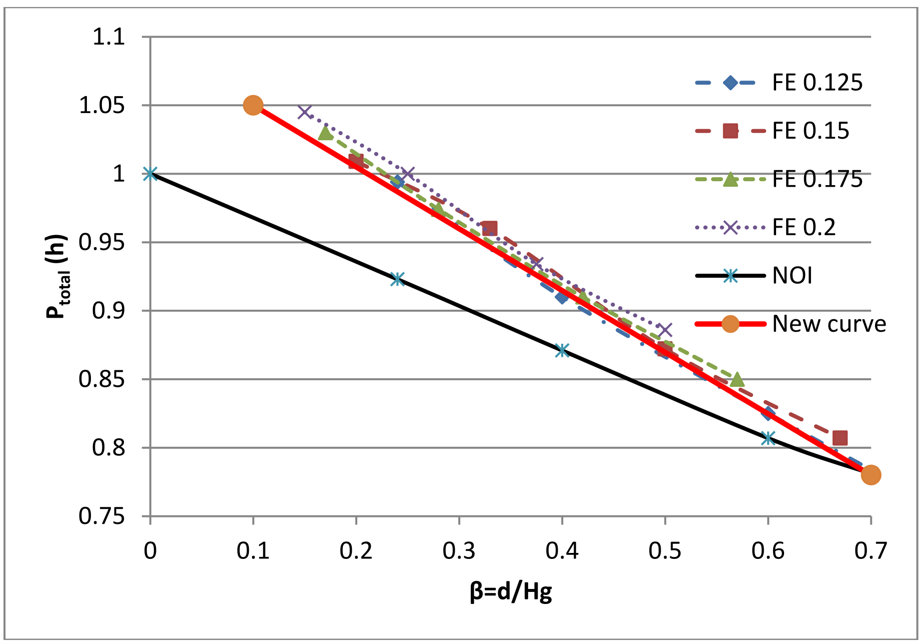

Figure 6. Calibration of "new curve" based on FE analysis results for total hydrodynamic load on vertical gate set back from the vertical face of a rigid dam.

CONCLUSION

Several conclusions can be made from the study on the hydrodynamic loads on spillway gates induced during earthquakes. First, the location of the spillway gate in respect to the dam face has significant influence on the pressure level developed at the gate skinplate. The study shows that pressure reduction is observed as the crest spillway gate is set back from the face of the gravity dam. Some other important factors under investigation by the author of this paper that may have impact on the gate loads during earthquake are: curvature and slope of the gate skinplate, geometry of the upstream dam face, and flexibility of the dam and the gate structure.

The results in Figure 3 show that the Westergaard's approximate equation (9), commonly used in the engineering practice, overestimates the hydrodynamic loads induced during earthquakes at the upper part of the rigid dam, where the crest spillways are usually installed.

In the presented study, a formula was developed to determine seismically induced hydrodynamic loads on vertical spillway gates installed at rigid dams with the vertical upstream face. The approach is based on the exact Westergaard's solution with vertical gate set back from the dam face. Implemented in an Excel spreadsheet, the formula can be utilized in the preliminary seismic analysis and design of the spillway gates installed at gravity dams.

ACKNOWLEDGEMENTS

The author would like to express his sincere thanks to Dam Safety Office at Reclamation for supporting the research on seismic induced hydrodynamic loads on spillway gates.

REFERENCES

Chopra A. K. (1967), *Hydrodynamic Pressures on Dams during Earthquakes*, Journal of the Engineering Mechanics Division, Proceedings of the ASCE, pp 205-223.

Chwang A. T., Housner G. (1977), *Hydrodynamic Pressures on sloping Dams during Earthquakes, Part 1 – Momentum Methods,* J. Fluid Mech. Vol. 87, Part 2, pp. 335-341.

Chwang A. T. (1978), *Hydrodynamic Pressures on sloping Dams during Earthquakes, Part 2 – Exact theory*, J. Fluid Mech. Vol. 87, Part 2, pp. 343-348.

Housner G. W. (1990), *The Momentum-balance Method in Earthquake Engineering*, Selected Earthquake Engineering papers of G.W. Housner, ASCE.

Nakayama Y., Ohmachi T., Inoue S. (1991), *Practical Evaluation of Hydrodynamic Pressures on Dam-Gates during Earthquake,* Proceeding of JSCE A, Vol. 64, No.4, pp. 959-969, 2008. (in Japanese).

Salamon J.W. (2011), *Seismic Induced Loads on Spillway Gates - Literature Review*, Bureau of Reclamation, DSO-11-06 Report, Denver, Colorado.

Sasaki T., Iwashita T., Yamaguchi Y. (2007), *Calculation Method of Hydrodynamic Pressure in Seismic Response Analysis of Gates*, Technical Report on the 39th Joint Meeting May 2007, Panel on Wind and Seismic Effects, Tsukuba, Japan.

Todd R.V. (2002), *Determining Earthquake Loading on Spillway Gates*, Hydro Review, Volume XXI, No.4, pp 92-99.

USACE (2003), U.S. Army Corp of Engineers, *EM 1110-2-6051 – Time-History Dynamic Analysis of Concrete Hydraulic Structures*, December 2003.

Westergaard H. M. (1931), *Water Pressures on Dams during Earthquakes*, ASCE Transactions, pp. 418-433, November 1931.

Von Karman T. (1931), *Discussion on: Water Pressures on Dams during Earthquakes by Westergaard*, ASCE Transactions, pp. 434-436, November 1931.

Zanger C. N., (1952), *Hydrodynamic pressures on Dams due to horizontal Earthquake Effects*, Bureau of Reclamation, Engineering Monograph No.11.

NUMERICAL ASSESSMENT OF HYDRODYNAMIC LOADS INDUCED DURING SEISMIC INTERACTION BETWEEN RESERVOIR AND CONCRETE DAM

Jerzy Salamon, P.E., Ph.D.[1], Jonna Manie, M.Sc.[2]

ABSTRACT

During the 2016 Monticello Blind Prediction Analysis Workshop hosted by the USSD Earthquake Committee, the Monticello Dam case study was investigated. Participants in the study attempted to generate finite element (FE) results using various methods to determine seismically induced hydrodynamic loads on the concrete arch dam. The primary methods were based on the "added mass" approach, as well as the "acoustic fluid" and the "fluid-like material model" analysis techniques. Among the results presented in the workshop, significant differences were observed for all methods.

This paper presents a comparative analysis of these three methods. This comparison is illustrated using the results of FE analysis on two concrete gravity dams, one of small size and one of medium size. This paper also discusses the assumptions and limitations of the analysis techniques.

INTRODUCTION

The hydrodynamic loads induced during earthquakes are important for the design and structural evaluation of concrete dams. An in-depth understanding of the computation methods and their limitations are the key factor that determines the accuracy of the analysis results.

In this paper, seismic interactions between a reservoir and a concrete gravity type dam are investigated. Three approaches commonly used in the direct time integration analysis are presented and discussed: (1) the "added mass" approach, (2) the "acoustic fluid" analysis technique, and the (3) "fluid-like material model" method.

ADDED MASS APPROACH

General

The first systematic analysis of dam-reservoir interaction was performed by Westergaard [5] in connection with the Bureau of Reclamation's design of Hoover Dam. In a study of the earthquake response of a rigid dam with a vertical upstream face (Figure 1), Westergaard developed an analytical solution for the hydrodynamic pressure distribution

[1]Technical Specialist, Waterways & Concrete Dams Group, Bureau of Reclamation, PO Box 25007, Denver, Colorado, 80225, USA, e-mail: jsalamon@usbr.gov
[2]Consulting Engineer, Engineering Team, DIANA FEA BV, Delftechpark 19a, 2628 XJ, Delft, The Netherlands, e-mail: j.manie@dianafea.com

in the reservoir and along the upstream face of the dam, as a result of the dam harmonic horizontal motions. The approximate formula for the parabolic hydrodynamic pressure distribution over a vertical dam face, and the concept of added mass presented by Westergaard in a fundamental and in a simplistic form, have been used consistently in the engineering practice for the preliminary analysis and design of concrete dams.

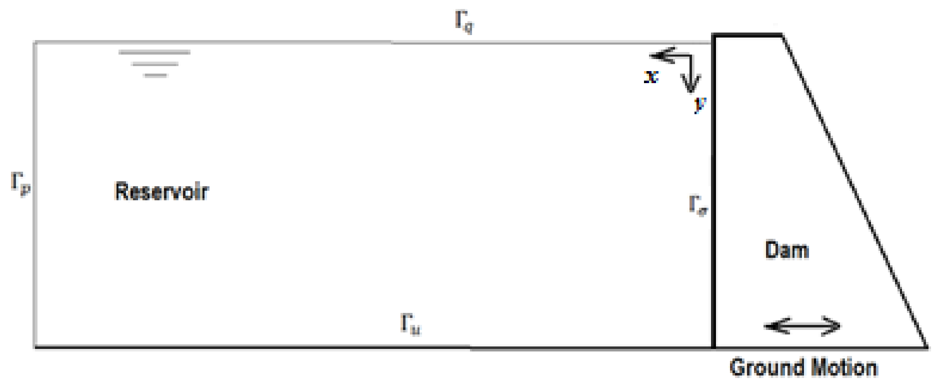

Figure 1. Westergaard's model.

<u>Problem Formulation</u>

The seismic motion of a rigid dam interacting with an infinite length reservoir of depth *h* was mathematically described by Westergaard [5] in terms of the theory of elasticity of solids, based on the formulation provided by Lamb [2]. The boundary value problem (BVP) was formulated by Westergaard in the following form:

Equations of Motion:

$$\frac{\partial \sigma}{\partial x} = \frac{w}{g}\frac{\partial^2 u}{\partial t^2} \qquad \frac{\partial \sigma}{\partial y} = \frac{w}{g}\frac{\partial^2 v}{\partial t^2} \tag{Eq.1}$$

Geometric Equation:

$$\varepsilon_{xy} = \frac{1}{2}\left(\frac{\partial u}{\partial y} + \frac{\partial v}{\partial x}\right) \tag{Eq.2}$$

Constitutive Law for Reservoir:

$$p = \frac{1}{3}\sigma_{kk} = K\,\varepsilon_{kk} \tag{Eq.3}$$

where: *u*, *v* are horizontal and vertical displacements, respectively
x is the axis at the surface of the reservoir directed upstream (Figure 1)
y is the vertical downward axis (Figure 1)
p is the pressure in the reservoir
σ_{kk} *and* ε_{kk} are volumetric stress and volumetric strain, respectively
w is the weight of water per unit of volume
g is the acceleration due to gravity
K is the bulk modulus of water

The model in his original form was defined with the following assumptions:

- The dam upstream face is straight and vertical at Γ_σ.
- The dam does not deform and is considered to be a rigid block.
- The reservoir is infinite in length at Γ_p.
- Dam sinusoidal oscillations are horizontal.
- Small motions are assumed during earthquake.
- The problem is defined in two-dimensional (2D) space.
- The period of free vibration of the dam, T_0, is significantly smaller than the period of vibration, T, of the earthquake (resonance is not expected).
- Nondimensional horizontal acceleration of $\alpha = 0.1$.
- Horizontal harmonic ground/dam motion applied to the dam.

Exact and Approximate Solutions

Westergaard addressed the problem of horizontal and vertical motions of water (plane strain) in the form of a stress (pressure) distribution in the reservoir and along the upstream face of the dam. The maximum pressure distribution at the upstream face of the dam was expressed by the equations:

$$p = \frac{8\alpha wh}{\pi^2} \sum_{1,3,5\ldots}^{n} \frac{1}{n^2 c_n} \sin \frac{n\pi y}{2h} \qquad \text{(Eq.4)}$$

with:

$$c_n = \sqrt{1 - \frac{16wh^2}{n^2 gkT^2}} \qquad \text{(Eq.5)}$$

where:

h is the depth of the reservoir
α is the maximum horizontal acceleration of dam divided by g
T is the period of horizontal vibration at the dam

Westergaard obtained the approximate solution by approximation of the exact solution (Eq.4 and Eq.5) using a parabolic function expressed by Eq.6:

$$p = \frac{7}{8} w\alpha\sqrt{h(h-y)} \qquad \text{(Eq.6)}$$

Concept of Added Mass

The parabolic hydrodynamic pressure distribution over the height of the dam was determined by Westergaard to be the same as a pressure developed by a certain body of water called "*added mass*," which was forced to move with the dam during the ground motion. The volume of water of "*added mass*" per unit width was described by a parabola (Figure 2) with dimension b expressed by Eq.7:

$$b = \frac{7}{8} w \sqrt{h(h-y)} \qquad \text{(Eq.7)}$$

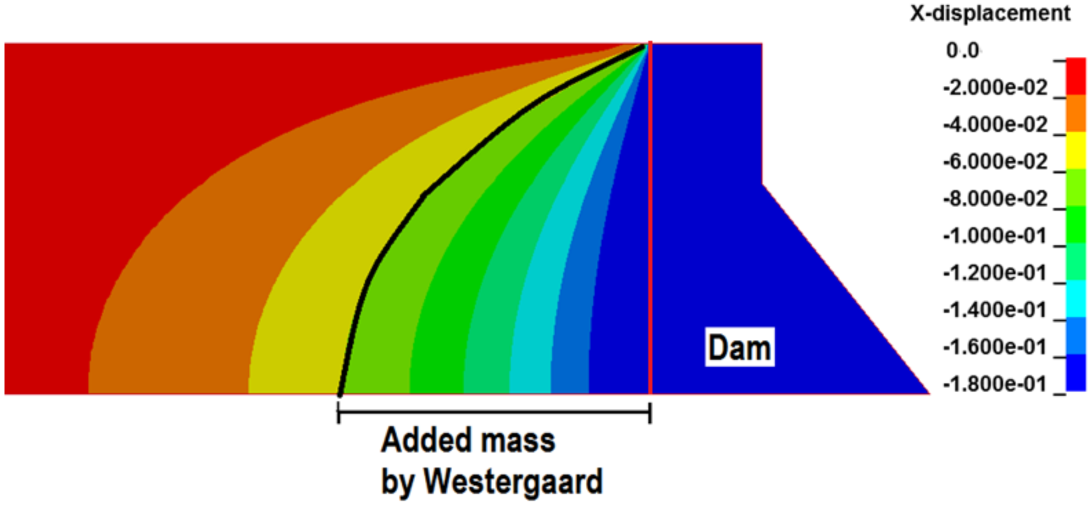

Figure 2. Horizontal displacement of a rigid dam obtained in FE analysis for a 100-feet-deep reservoir. Black line denotes the area of *added mass* volume determined by Westergaard (Eq.7).

DIRECT TIME INTEGRATION METHODS

General

This section presents a brief overview of the direct time integration methods used to calculate the seismically induced hydrodynamic pressures at the face of a concrete gravity dam using the FE analysis method. Two approaches are presented: (1) the classical "acoustic fluid" approach, and (2) the "fluid-like material model" approach.

Coupling of Acoustic Fluid and Structural Elements

In this method, the displacement field of the dam (structural domain) is coupled with the pressure field of the reservoir (fluid domain) via the interaction forces at the interface between the dam and the reservoir (Figure 3).

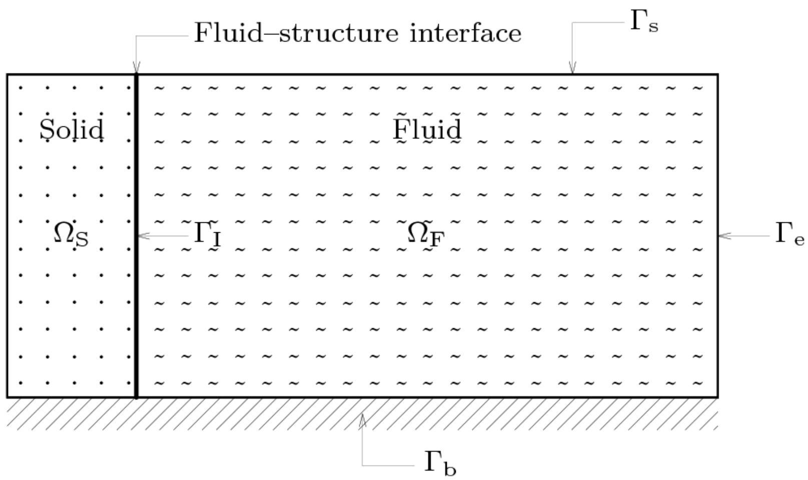

Figure 3. Acoustic fluid model.

In the structural domain Ω_S, the discretization in the familiar form is given by:

$$M_S\ddot{u} + C_S\dot{u} + K_S u + f_I = f_S^{ext} \quad \text{(Eq.8)}$$

where: M_S, C_S, and K_S are mass, damping, and stiffness matrices, respectively
u is a set of unknowns describing the displacements of the structure
f_I stands for forces due to the interface interaction with the fluid
f_S^{ext} represents external forces

The dynamic pressure distribution in the fluid is described by a single variable p. Assuming the state of the fluid is linear, the governing equation is the wave (acoustic) equation:

$$\nabla^2 p = \frac{1}{c^2}\ddot{p} \quad \text{(Eq.9)}$$

where p is the dynamic pressure (compression positive)
c is the wave speed given by:

$$c^2 = \frac{\beta}{\rho_F} \quad \text{(Eq.10)}$$

where β is the bulk modulus
ρ_F is the fluid density

Coupling within the dam and the reservoir is achieved by considering the interface forces at the dam face. The conditions applying to the fluid-structure interface Γ_I can be written as:

$$\sigma\, n_S = p\, n_F \quad \text{(Eq.11)}$$

where n_F and n_s are the outward normal to the fluid domain and the outward normal to the structural domain, respectively.

Coupling between the fluid domain and the structural domain can be achieved by continuity between the normal displacements with the condition $u_F = u_S$ and is obtained by combining this condition with Eq.11:

$$\frac{\partial p}{\partial n} = -\rho_F \mathrm{n_F}^{\mathrm{T}} \ddot{\mathrm{u}}_{\mathrm{S}} \quad \text{(Eq.12)}$$

At the free surface, Γ_s, and the fluid far field boundary (infinite extent), Γ_e, the prescribed dynamic pressures are assumed zero. For the bottom boundary, Γ_b, a full reflective bottom is assumed (i.e., no bottom absorption effects or prescribed dynamic pressures).

Implementing a standard FE discretization for approximating p, a system of algebraic equations for the fluid domain can be defined by:

$$M_F \ddot{p} + K_F p + r_I = 0 \quad \text{(Eq.13)}$$

where M_F and K_F are the fluid mass and stiffness matrixes, respectively
r_I is the interface reaction force

The interface interaction forces within the fluid element can be written as:

$$f_I^e = -R^{eT} p^e \quad \text{(Eq.14)}$$

where R^e is the interaction matrix for the dynamic pressures on the element level.

Likewise, the contribution r_I on element level as:

$$r_I^e = \rho_F R^e \ddot{u}^e \quad \text{(Eq.15)}$$

After assembling contributions from each type of element, the following coupled system of equations for the fluid structure interaction problem is obtained:

$$\begin{bmatrix} M_S & 0 \\ \rho_F R & M_F \end{bmatrix} \begin{Bmatrix} \ddot{u} \\ \ddot{p} \end{Bmatrix} + \begin{bmatrix} C_S & 0 \\ 0 & 0 \end{bmatrix} \begin{Bmatrix} \dot{u} \\ \dot{p} \end{Bmatrix} + \begin{bmatrix} K_S & -R^T \\ 0 & K_F \end{bmatrix} \begin{Bmatrix} u \\ p \end{Bmatrix} = \begin{Bmatrix} f_S^{ext} \\ 0 \end{Bmatrix} \quad \text{(Eq.16)}$$

If the compression effects are neglected (i.e., an incompressible fluid is assumed ($c = \infty$)), the fluid matrix M_F becomes zero. The dynamic pressure vector $\boldsymbol{p}$ can now be obtained directly in terms of $\ddot{u}$ as:

$$\boldsymbol{p} = -K_F^{-1} \rho_F R \ddot{u} \quad \text{(Eq.17)}$$

Substituting Equation 17 in Equation 16, the structural matrix results in the following general equation:

$$\left(M_S + \widetilde{M}_F\right)\ddot{u} + C_S\dot{u} + K_S u = f_S^{ext} \qquad \text{(Eq.18)}$$

where the added mass is simply given by:

$$\widetilde{M}_F = \rho_F R^T K_F^{-1} R \qquad \text{(Eq.19)}$$

If an arbitrary transient loading is considered, the response of the model with incompressible fluid is obtained by a direct time integration method.

The "acoustic fluid" formulation is evaluated in this study using DIANA FE software developed by DIANA FEA BV [4].

<u>Fluid-Like Behavior Model</u>

Modeling fluid behavior with a "fluid-like" material model is an alternative approach for analyzing the fluid-structure interaction behavior. The fluid is defined in the BVP as a structural elastic material (Eq.20) with the shear modulus equal to zero.

<u>Constitutive Law for Fluid:</u>

$$\dot{p} = \tfrac{1}{3}\,\dot{\sigma}_{kk} = K\,\dot{\varepsilon}_{kk} \qquad \text{(Eq.20)}$$

where: $\dot{\varepsilon}, \dot{\sigma}, and\ \dot{p}$ are strain, stress, and pressure rates
K is the bulk modulus of fluid

The behavior of the fluid-like material model is implemented in LS-DYNA FE software developed by LSTC [3].

CASE STUDIES

<u>General</u>

To illustrate the analysis techniques discussed above, two models of the concrete dams are considered: (1) a small 100-foot-high dam, and (2) a medium 287-foot-high dam (Figure 4).

The foundation in the models has a length of 1200 feet and a depth of 300 feet. The foundation is modeled massless with linear elastic material properties. The water level is 100 feet for the small dam and 282 feet for the medium dam. The reservoir has a length of 600 feet for both dam models.

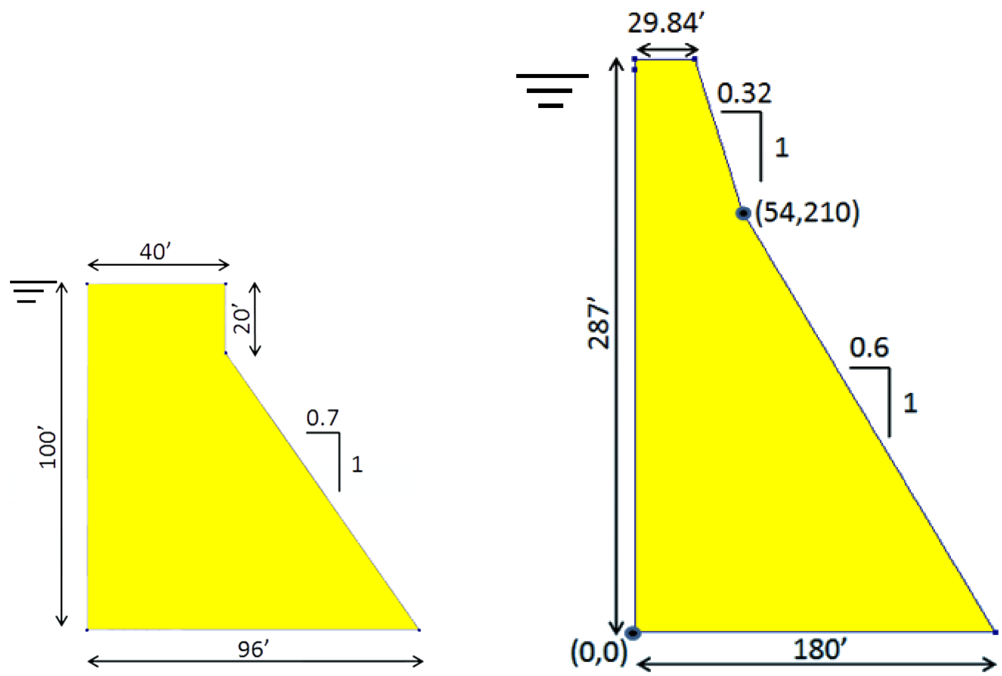

Figure 4. Model of small dam (left) and medium dam (right).

Description of the FE Model

The FE models are set up with plane strain elements. At the free surface and the fluid far field boundary (infinite extent), the prescribed pressures are assumed zero. For the reservoir bottom, a full reflective boundary is assumed (i.e., no bottom absorption effects or prescribed dynamic pressures). Table 1 lists the material properties used in the analysis for the dam, foundation, and reservoir.

Table 1. Material properties.

Material property	Dam	Foundation	Reservoir	Unit
Young's modulus E	4.0E6	3.0E6	3.0E5*	lb/in²
Poisson's ratio ν	0.2	0.2	-	-
Density ρ	155.0	0.0	62.4	lb/ft³
Sonic speed c_w	-	-	4869.0	ft/s

Note (*) – Bulk modulus

The amplitude of the excitation (i.e., prescribed harmonic acceleration in horizontal direction) was 0.1 g and was applied at the base of the dam for the model with a rigid foundation, and at the bottom and sides of the foundation block for the model with the elastic properties of the foundation. The harmonic excitations at 0.66 second and 1.33 seconds were considered in the analysis.

Modal Analysis

The ratio of the natural frequency of the reservoir to the natural frequency of the dam is the key parameter determining the effect of the reservoir compressibility in the reservoir-dam interaction during an earthquake [1]. The first natural frequency of the reservoir can be determined by the equation:

$$f_r = \frac{c_w}{4\,h} \qquad \text{(Eq.21)}$$

For reservoir depths of 100 feet and 282 feet, assumed for the small dam and medium dam models in Figure 4, respectively, the natural frequencies of the reservoir determined from Eq. 21 are 12.18 Hz and 4.32 Hz, respectively.

Four eigenfrequencies for the small size dam and medium size dam models are presented in Tables 2 and 3. The frequencies were determined by free-vibration eigenvalue analyses for the empty reservoir, added mass, and incompressible fluid case, and by a direct frequency response method for the compressible fluid case, considering elastic and rigid foundations.

Table 2. Eigenfrequencies [Hz] for small size dam.

Reservoir	Foundation	1st	2nd	3rd	4th
Empty reservoir	rigid	13.1	32.0	33.9	61.8
Empty reservoir	elastic	8.2	15.2	21.6	43.4
Added mass	rigid	11.5	28.7	32.2	50.9
Added mass	elastic	7.1	15.1	19.1	39.1
Incompressible fluid	rigid	11.9	30.2	32.4	58.9
Incompressible fluid	elastic	7.3	15.1	20.1	42.4
Compressible fluid	rigid	11.0	28.7	31.5	50.1
Compressible fluid	elastic	7.1	15.1	20.7	42.2

Table 3. Eigenfrequencies [Hz] for medium size dam.

Reservoir	Foundation	1st	2nd	3rd	4th
Empty reservoir	rigid	3.9	10.0	12.9	18.6
Empty reservoir	elastic	2.9	7.1	8.1	13.2
Added mass	rigid	3.0	7.8	12.8	14.3
Added mass	elastic	2.3	6.0	7.8	11.2
Incompressible fluid	rigid	3.2	8.6	12.8	17.0
Incompressible fluid	elastic	2.4	6.5	7.8	13.1
Compressible fluid	rigid	3.1	5.0	7.3	9.4
Compressible fluid	elastic	2.4	4.9	6.6	12.3

The results presented in Tables 2 and 3 show that the eigenfrequencies of the dam- reservoir-foundation system vary significantly with the type of the dam-reservoir-foundation model considered in the analysis. The highest natural frequency is obtained for the elastic dam model on rigid foundation without the presence of the reservoir. Note that elasticity of the foundation is a significant factor influencing the natural frequency of the dam-reservoir-foundation system.

Table 4 presents the ratio between natural frequencies of the reservoir and natural frequencies of the dam-reservoir-foundation model.

Table 4. Ratio between the first natural frequencies of the reservoir and the dam-reservoir-foundation model.

Reservoir	Foundation	Small Size Dam	Medium Size Dam
Empty reservoir	rigid	0.93	1.11
Empty reservoir	elastic	1.49	1.49
Added mass	rigid	1.06	1.44
Added mass	elastic	1.72	1.87
Incompressible fluid	rigid	1.02	1.35
Incompressible fluid	elastic	1.67	1.80
Compressible fluid	rigid	1.11	1.39
Compressible fluid	elastic	1.72	1.80

In general, the first natural frequency of the reservoir is higher than that of the dam-reservoir-foundation system of the two dam models (Figure 4) selected in the analysis (ratio larger than 1.0 in Table 4).

Analysis of a Rigid Dam on a Rigid Foundation

The classical model of a rigid dam placed on a ridged foundation is evaluated in this section. Water pressure distributions at the face of the rigid dam, obtained by both the approximate and the exact Westergaard's solutions [5], are compared in Figure 5 with the "fluid-like material model" FE analysis results for the small size dam (Figure 4).

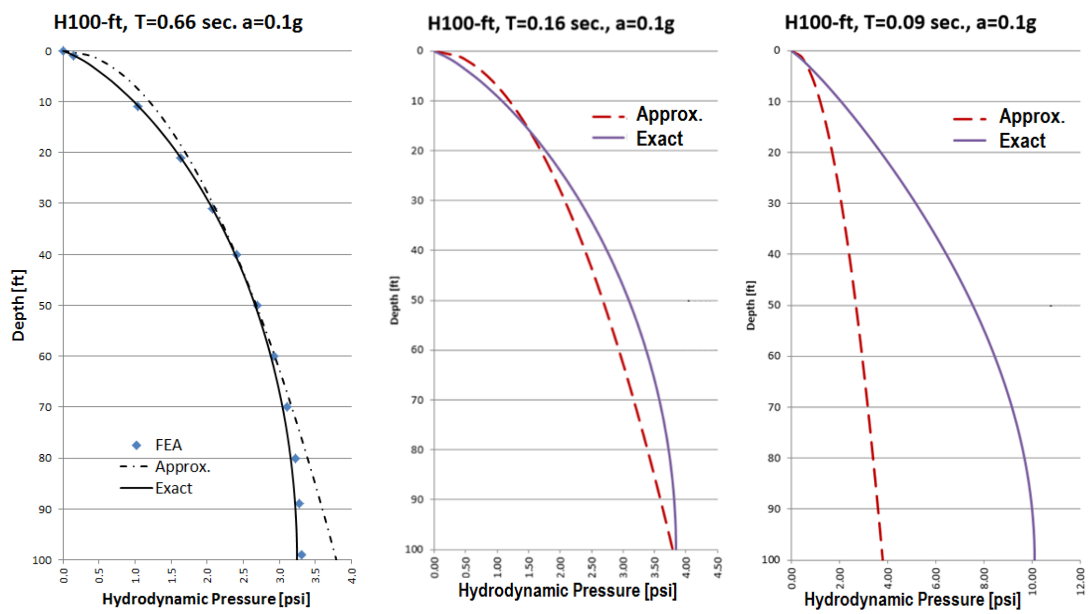

Figure 5. Hydrodynamic pressures at the face of a rigid dam obtained by exact and approximate Westergaard's solutions for the harmonic dam excitations at periods of 0.66 second (1.52 Hz), 0.16 second (6.25 Hz), and 0.09 second (11.1 Hz) and the acceleration amplitude of 0.1g.

In general, the approximate Westergaard's formula (Eq. 6) overestimates the hydrodynamic pressure at the upper part of a rigid dam when it is compared with the exact Westergaard's solution. The increase in the hydrodynamic pressure determined by the exact Westergaard's solution (Figure 5, right graph) could be explained by resonance between the reservoir (first natural frequency of 12.18 Hz) and the dam excitation frequency of 11.1 Hz. Note, that the Westergaard's solution is valid only if the frequency of excitations is significantly smaller than the first natural frequency of the reservoir. For comparison, FE analysis results are presented in Figure 5 (left), excluding higher frequency wave effects in the reservoir.

Time Analysis

The time analyses were performed using the "fluid-like material model" approach [3], assuming various arrangements for the dam-reservoir-foundation system. A rigid foundation was assumed for both analysis models and the harmonic excitation of the dam at periods of 0.66 second and 1.33 seconds. Figures 6 and 7 present time-history pressure distributions for both the small-size and medium-size dam models. These graphs illustrate a pressure at the dam face resulting from combining the dam excitation effect and the wave's generated by the reservoir compressibility. When higher frequency wave effects in the reservoir are excluded, the pressure as a function of time would be a sinusoidal function, with the frequency corresponding to the frequency of excitation. The local peaks in the pressure distribution (Figure 6) are separated by 0.81 second, which corresponds to the reservoir first natural frequency of 12.18 Hz (period 0.82 second) determined by Equation 21.

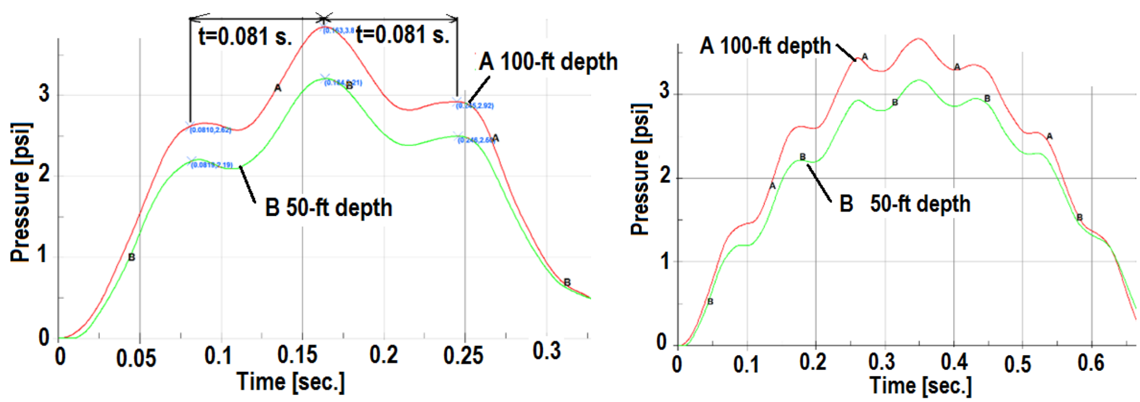

Figure 6. Pressure distribution at the dam face for small size dam with a rigid foundation at 100-foot and 50-foot reservoir depths and for the harmonic excitation at 0.66 second (left) and 1.33 seconds (right).

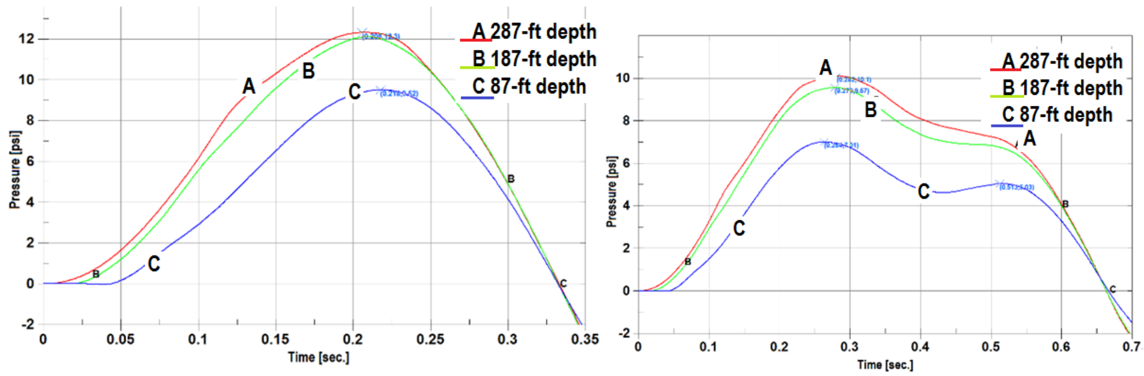

Figure 7. Pressure distribution at the middle size dam face with the rigid foundation at 287-, 187-, and 87-foot depths and for the harmonic excitation at 0.66 second (left) and 1.33 seconds (right).

The maximum pressures obtained from the FE analysis are compared with Westergaard's solutions in Table 5. The results show that higher pressures are obtained when the compressibility effect is included in the analysis.

Table 5. Comparison of maximum pressures at the bottom of the reservoir [lb/in^2]

Reservoir	Foundation and Period	Small Size Dam	Medium Size Dam
Incompressible fluid	rigid	3.43	9.79
Incompressible fluid	elastic	3.76	11.43
Compressible fluid	rigid & (T=0.66 sec.)	3.85	12.3
Compressible fluid	rigid & (T=1.33 sec.)	3.67	10.1
Westergaard approximate solution		3.79	7.58
Westergaard exact solution	T=0.66 sec.	3.25	6.68
	T=1.33 sec.	3.23	6.49

Figures 8 and 9 show the positive and the negative hydrodynamic pressures turbulence that develops in the reservoir during simulation of the dam-reservoir model at the various analysis times. Pressure waves that separate from the face of the dam spread along the length of the reservoir until they are absorbed by the "far field boundary conditions" (Perfect Matching Layers [3]). The turbulence in the pressure distribution is observed in the analysis for the linear material model with harmonic dam excitations and geometric non-linearities (large deformations).

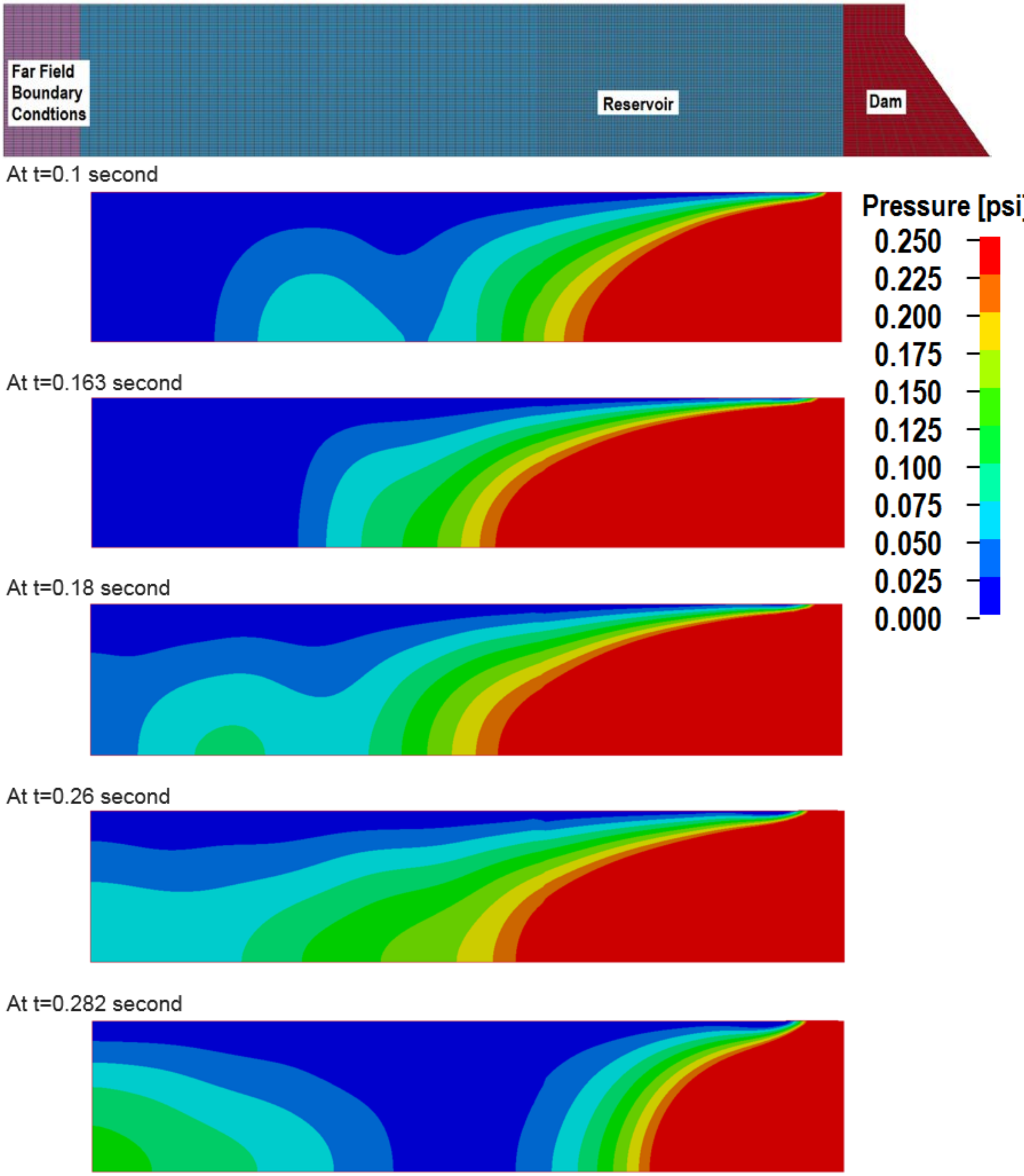

Figure 8. Positive pressure distribution in the reservoir corresponding to the time line presented in Figure 6 (left).

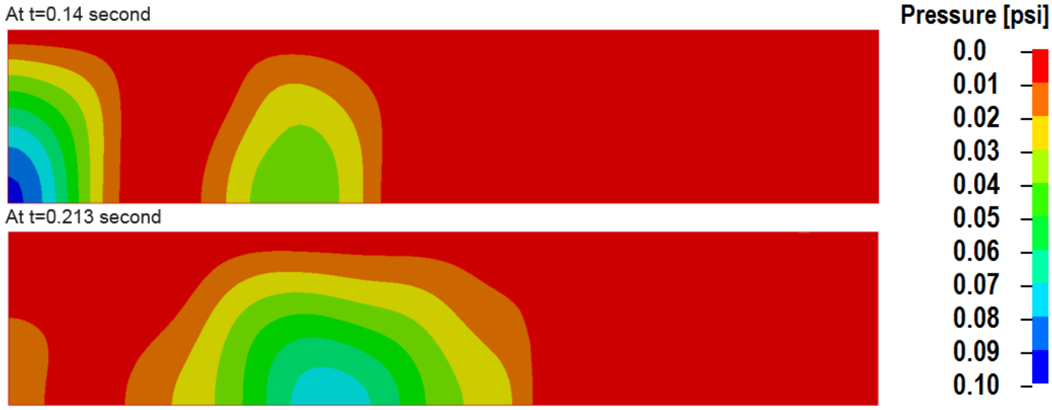

Figure 9. Negative pressure distribution in the reservoir corresponding to the time line presented in Figure 6 (left).

SUMMARY AND CONCLUSIONS

Summary

This paper evaluates three analysis methods that are commonly used in the time simulations of the dam-reservoir-foundation system during an earthquake. These methods include: (1) the "added mass" approach, (2) the "acoustic fluid" method, and (3) the "fluid-like material model" method. The theory for each of the methods is briefly presented and is illustrated by the results of two analyzed concrete dams: the small size dam and the medium size dam. In general, the results of the analysis could be summarized as follows:

- A good agreement existed between the exact Westergaard's solution and the FE results for a rigid dam with vertical upstream dam face when higher frequency wave effects are excluded from the analysis; however, the hydrodynamic pressure determined by the approximate Westergaard's solution significantly differs from the results obtained by the FE and the exact Westergaard's solutions.
- According to analysis results, eigenfrequencies of the dam-reservoir-foundation system vary significantly with the type of assumptions made for the physical model.
- The FE time-history simulation of a linear dam-reservoir model with harmonic dam excitations showed that compressibility of the fluid significantly influences the analysis results, resulting in a turbulent pressure distribution in the reservoir.

Conclusions

The following conclusions could be formulated based on the results of the investigations:

- The differing results of the blind predictions in the Monticello Dam analysis appear to be due primarily the various approaches used by participants. Of the three approaches, the "added mass" approach offers the least confidence for accuracy of the solution.

- The “added mass” approach, based on the approximate Westergaard’s solution, only roughly estimates the mass of water interacting with the dam during an earthquake. The error is particularly large when the excitation frequency is similar to the first natural frequency of the reservoir. Even greater errors would exist in Westergaard’s solution if the dam face was not vertical, or if the dam and the foundation is considered not rigid.
- It appears that the “added mass” approach should not be implemented in the advanced time-history analysis, and that it only be used in a preliminary estimation of seismically induced hydrodynamic loads on dams.
- The “added mass” may provide relatively good results only for “rigid” type dams (small size concrete gravity dams on stiff rock foundations) with vertical upstream face.
- Compressibility of water is the primary factor that influences the hydrodynamic pressure distribution in the reservoir. The time analysis with an “incompressible fluid” material model provides significantly different results when compressibility of the fluid is considered.
- It appears that a hybrid frequency-time domain analysis should be implemented in the seismic simulations of the dam-reservoir-foundation system.

REFERENCES

[1] Chopra A. K., *Hydrodynamic Pressures on Dams during Earthquakes*, Journal of the Engineering Mechanics Division, Proceedings of the ASCE, 1967.

[2] Lamb H., *Hydrodynamics*, Fifth Ed., Chapter X, 1924.

[3] LSTC, LS-DYNA Manual, Livermore 2013.

[4] Manie J. (Ed.), DIANA User’s Manual, Delft 2016.

[5] Westergaard H. M., *Water Pressures on Dams during Earthquakes,* ASCE Transactions, November 1931.